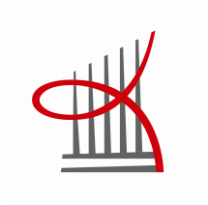

EXPRESSION OF miR-32, Ki-67, Btg2, AND Pten IN TRANSGENIC MOUSE PROSTATE TISSUE

Osku Alanen

Bachelor's Thesis
November 2014
Degree Programme in
Laboratory Sciences

TAMPEREEN AMMATTIKORKEAKOULU
Tampere University of Applied Sciences

ABSTRACT

Tampereen ammattikorkeakoulu
Tampere University of Applied Sciences
Degree Program in Laboratory Science

ALANEN, OSKU:
Expression of miR-32, Ki-67, Btg2, and Pten in Transgenic Mouse Prostate Tissue

Bachelor's thesis 64 pages, appendices 2 pages
November 2014

Prostate cancer is the most common type of cancer found in men. An advanced form of the cancer – castration-resistant prostate cancer – is responsible for over 28 000 deaths in the United States every year with no current curative treatments available. As a result, new biomarkers and treatments are desperately needed. Putative biomarkers include, for example, certain microRNAs – small non-coding RNAs that are involved in the regulation of gene expression – or tumor suppressor genes that are responsive for cell cycle regulation. The objective of the thesis was to investigate the expression of several biomarkers in transgenic mouse prostate tissue. The purpose was to establish protocols for the *in situ* hybridization of miR-32, and immunohistochemical staining methods for Ki-67, Btg2, and Pten – and to investigate their expression in transgenic mouse prostate tissue.

During this thesis, a successful protocol for the immunohistochemistry of Ki-67, Btg2, and Pten with PAXgene fixation was established. A working protocol for the *in situ* hybridization of miR-32 was also established, but with inconsistent staining. A low level of miR-32 expression was detected in the dorsolateral lobe of both wild type (WT) and transgenic (TG) prostates. Ki-67 was shown to have a low expression in both WT and TG prostates. Btg2 was expressed mainly in the basal cells of both WT and TG prostates, including the urethra and ductus deferens. Similarily, Pten expression was observed in the basal cells of both WT and TG urethra and, additionally, in the prostate. All biomarkers had close to identical expression in both WT and TG prostates.

In conclusion, the protocol established here for the immunohistochemistry of Ki-67, Btg2, and Pten is sufficient for further use with commercial PAXgene fixation. However, the immunohistochemistry here should be repeated with fresh tissue sections, in order to ensure consistent staining of all sections. Further optimization should be attempted with *in situ* hybridization before moving into samples with confirmed prostatic lesions. In the future, the protocol established here for Ki-67, Btg2, and Pten can be used in mouse samples with confirmed prostatic lesions in order to help evaluate their role in prostate carcinogenesis, and in the formation of castration resistance.

Key words: prostate cancer, biomarker, *in situ* hybridization, immunohistochemistry

TIIVISTELMÄ

Tampereen ammattikorkeakoulu
Laboratorioalan koulutusohjelma

ALANEN, OSKU:
miR-32:n, Ki-67:n, Btg2:n ja Pten:n ilmentyminen transgeenisen hiiren eturauhaskudoksessa

Opinnäytetyö 64 sivua, joista liitteitä 2 sivua
Marraskuu 2014

Eturauhassyöpä on miesten yleisin syöpä. Kastraatioresistentti eturauhassyöpä on eturauhassyövän edistynyt muoto, johon ei ole löydetty parantavaa hoitokeinoa. Kastraatioresistentti eturauhassyöpä on vastuussa yli 28 000 kuolemasta vuosittain USA:ssa. Tästä johtuen uusia biomarkkereita ja hoitokeinoja etsitään jatkuvasti. Mahdollisia biomarkkereita voivat olla esimerkiksi mikroRNA:t, jotka ovat geenien ilmentymistä säätteleviä lyhyitä ei-koodaavia RNA:ita. Biomarkkereihin voivat kuulua myös eri tuumorisuppressorigeenit, jotka ovat osa solusyklin säätelyä. Opinnäytetyön tavoitteena oli tutkia useiden eri biomarkkerien ilmentymistä transgeenisen hiiren eturauhaskudoksessa. Opinnäytetyön tarkoituksena oli pystyttää *in situ* hybridisaatio -menetelmä miR-32:n määritykseen sekä menetelmä Ki-67:n, Btg2:n ja Pten:n immunohistokemiallista värjäystä varten ja tutkia pystytettyjen menetelmien perusteella näiden biomarkkerien ilmentymistä.

Ki-67:n, Btg2:n ja Pten:n määritystä varten pystytettiin yleispätevä immunohistokemiallinen värjäysmenetelmä PAXgene-fiksauksella. Lisäksi pystytettiin menetelmä miR-32:n määritykseen *in situ* hybridisaation avulla, mutta saatu värjäystulos oli epätasaista. *In situ* hybridisaation tulosten perusteella miR-32 ilmentymistä oli havaittavissa villityypin (WT) ja trasgeenisen (TG) hiiren dorsolateraalisessa eturauhaskudoksessa. Ki-67 ilmentyi pienissä määrin WT- ja TG-hiirten dorsaalissa eturauhaskudoksessa. Btg2 ilmentyi lähinnä WT- ja TG-hiirten eturauhasen, virtsaputken ja siemenjohtimen basaalisoluissa. Pten ilmentyi WT- ja TG-hiirten virtsaputken basaalisoluissa ja heikosti eturauhaskudoksessa. WT- ja TG-hiirten ilmentymisessä ei havaittu suurta eroa minkään biomarkkerin yhteydessä.

Opinnäytetyössä pystytetty immunohistokemiallinen värjäysmenetelmä on tarpeeksi luotettava jatkotutkimuksia varten. *In situ* hybridisaation tulosten parantamiseksi tulisi suorittaa lisää menetelmän optimointia. Lisäksi saadut immunohistokemialliset värjäykset tulisi toistaa tuoreemmilla kudosleikkeillä, jotta saataisiin selvitettyä syy mahdollisiin värjäyseroihin kudosleikkeiden välillä. Tulevaisuudessa opinnäytetyössä pystytettyjä menetelmiä voidaan käyttää hyödyksi eturauhassyöpää sairastavien hiirilinjojen tutkimisessa. Tutkimalla ilmentymistä näissä hiirilinjoissa voidaan arvioida näiden biomarkkerien roolia eturauhassyövän synnyssä sekä kastraatioresistentin eturauhassyövän muodostuksessa.

Asiasanat: eturauhassyöpä, biomarkkeri, *in situ* hybridisaatio, immunohistokemia

TABLE OF CONTENTS

ABBREVIATIONS AND TERMS

ABT	Avidin-biotin technique
AR	Androgen receptor
ARR2PB	Probasin promoter with two androgen response elements
AP	Anterior prostate
BCIP	5-bromo-4-chloro-3-indolyl phosphate
Btg2	B-cell translocation gene 2
CRPC	Castration resistant prostate cancer
DAB	3,3´-diaminobenzine tetrahydrochloride
DEPC	Diethylpyrocarbonate
DIG	Digoxigenin
DLP	Dorsolateral prostate
EDC	1-ethyl-3-(3-dimethylaminopropyl) carbodiimide
FFPE	Formalin-fixed paraffin embedded
H&E	Hematoxylin and Eosin
HIER	Heat-induced epitope retrieval
HRP	Horseradish peroxidase
ISH	*In situ* hybridization
LP	Lateral prostate
NBT	Nitro blue tetrazolium
PCa	Prostate cancer
PFA	Paraformaldehyde
PFPE	PAXgene-fixed paraffin embedded
PIA	Proliferative inflammatory atropy
PIN	Prostatic intraepithelial neoplasia
PSA	Prostate-specific antigen
PTEN	Phosphatase and tensin homolog
RISC	RNA-induced silencing complex
TG	Transgenic
VP	Ventral prostate
WT	Wild type
3′UTR	3′ untranslated region

1 INTRODUCTION

This bachelor's thesis was carried out in the Molecular Biology of Prostate Cancer Group, led by Professor Tapio Visakorpi at the Institute of Biosciences and Medical Technology (BioMediTech), University of Tampere. The research group is a part of the Prostate Cancer Research Center (PCRC) that investigates, for example, the development of aggressive prostate cancer and putative treatment options. The bachelor's thesis was supervised by Leena Latonen, Ph.D. The objective of this thesis is to study several putative biomarkers in transgenic mouse prostate tissue. To achive this, protocols for the *in situ* hybridization of miR-32 and for the immunohistohemistry of Ki-67, Btg2, and Pten will be established, and the expression of these putative biomarkers will be investigated during this thesis.

Prostate cancer – or prostate adenocarcinoma (PCa) – is a cancer of the prostate gland. Prostate cancer is the most common type of cancer found in men in the USA, with an estimation of around 233 000 new diagnoses and 29 480 deaths in 2014. It is estimated that around 1 in 7 men will be diagnosed with prostate cancer during their lifetime. (American Cancer Society 2014.) An advanced form of the cancer – castration-resistant prostate cancer (CRPC) – is accountable for over 28 000 deaths every year, emphasizing the need for finding effective treatment options and biomarkers for the detection of aggressive forms of the cancer (Nguyen et al. 2014).

The Molecular Biology of Prostate Cancer group has previously searched for several androgen-regulated microRNAs that may contribute in the development of prostate cancer and castration-resistant prostate cancer (CRPC). For this purpose, A transgenic mouse line expressing miR-32 in the prostate epithelium was created by the group. The expression of miR-32 can be studied with a technique called microRNA *in situ* hybridization, which visualizes the expression of a specific nucleic acid sequence inside a tissue (Nielsen 2012, 67). The other putative biomarkers, Ki-67, Btg2, and Pten, are proteins that are important for the proper functioning of the cell. Their expression can be researched with a technique called immunohistochemistry – a technique for visualizing the specific immunologic reaction of an antigen and an antibody in a tissue sample (Miller 2002, 421–423).

2 THEORETICAL BACKGROUND

2.1 Prostate cancer

2.1.1 Background

Prostate cancer (PCa) is a cancer of the prostate gland. The prostate gland is located between the rectum and the urinary bladder. Development of the prostate is dependent on androgens, such as testosterone, made in the testicles. The gland cells in the prostate are responsible for making the prostate fluid, which is added to the semen. A cancer of the gland cells of the prostate is called prostate adenocarcinoma. There are other possible cancers of the prostate, such as small cell carcinoma, but prostate adenocarcinoma is by far the most common. (American Cancer Society 2014.)

Prostate cancer is mainly diagnosed in men aged 65 or older, with the average age of 66 at the time of diagnosis (American Cancer Society 2014). In Finland, 4604 cases of prostate cancer were diagnosed in 2012 with age adjusted incidence of 81.2/100 000 (Finnish Cancer Registry 2014). For prostate cancer, there is an expected rise of + 24% in the annual number of cases by 2020 (Finnish Cancer Registry 2009). Figure 1 illustrates the mean annual number of cases of prostate cancer from 1961 onwards, with predictions up to 2020.

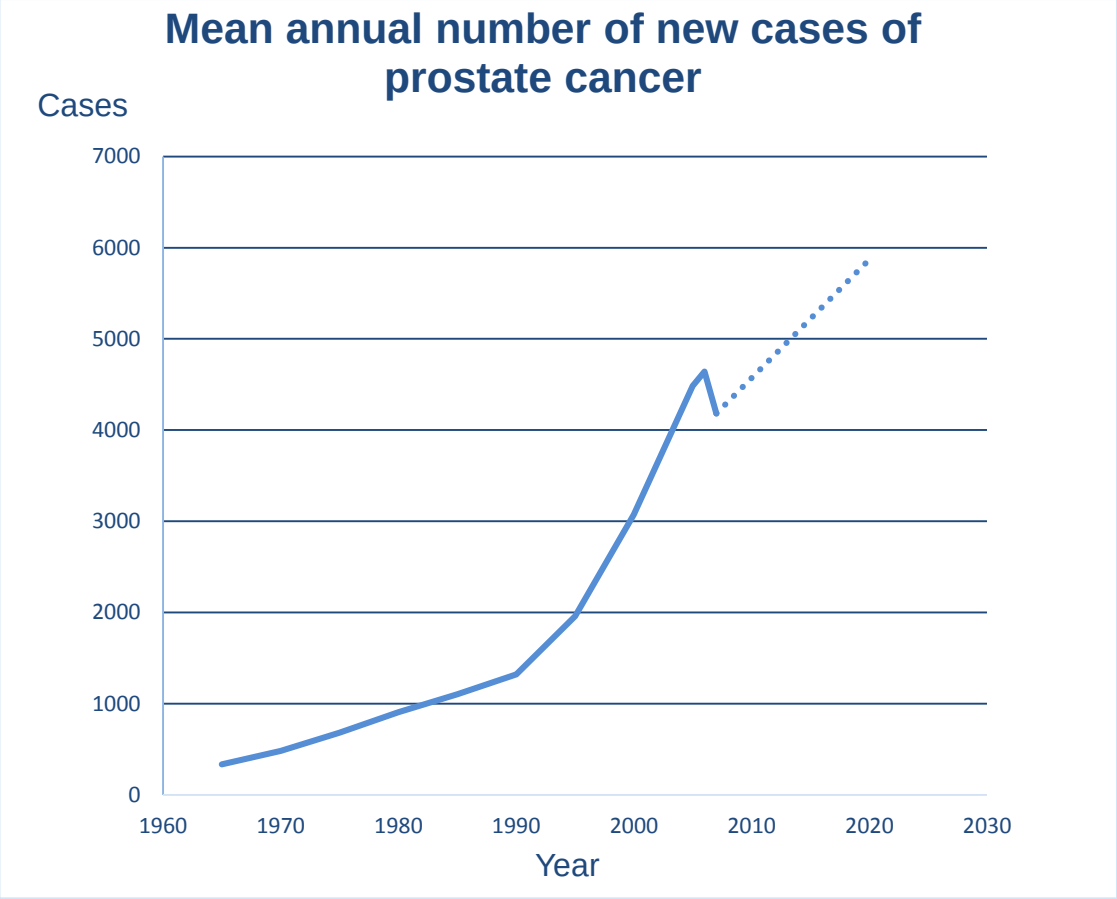

FIGURE 1. The mean annual number of new cases of prostate cancer. Predictions up to the year 2020 are included. Based on the data by Finnish Cancer Registry (2009)

2.1.2 Classification, diagnosis, and treatment

Currently, diagnosis of prostate cancer is dependent on histopathological or cytological examination of the prostate gland (Damber & Aus 2008). When a patient has elevated PSA, a prostate biopsy is recommended (Kawachi et al. 2010). The biopsy is performed under local anesthesia, with transrectal ultrasound to guide the biopsy needle (Damber & Aus 2008). The biopsy is graded with a Gleason score, which determines the aggressiveness of the cancer. The grading is based on hematoxylin & eosin stained sections of the biopsy sample, which are used to give a histologic score between two and ten. (Humphrey 2004.) In addition, PCa can be classified as a low-risk, intermediate-risk or a high-risk disease depending on the official classification (disease progression, PSA and Gleason score) (Damber & Aus 2008).

Treatment of prostate cancer is dependent on the progression of the disease; whether it's localized, locally advanced, or metastatic, has a rising PSA after surgery/radiation, or is hormone-resistant. However, the treatment options are usually limited to active surveillance, radical prostatectomy (surgery), radiotherapy, or hormonal therapy. (Damber & Aus 2008.) It is estimated that 80% of men with a Gleason score of eight to ten, who have undergone radical prostatectomy, will have a biochemical recurrence of prostate cancer at 15 years. These high-risk patients have a prostate cancer survival of 57% at 15 years. In comparison, patients with an organ-confined disease can reach survival rates of 90% at 15 years. (Pierorazio et al. 2010.) As the goal of radical prostatectomy is to remove all the cancerous prostate, PSA recurrence is a common indicator of cancer recurrence (Freedland & Moul 2007).

Hormonal therapy is usually the next step after PSA recurrence. Androgen deprivation therapy has been used since the 1940s for the treatment of advanced prostate cancer (metastatic). Possible treatment options include, for example, surgical castration, chemical castration, and estrogens. Blocking the effect of androgens on the prostate with anti-androgens is also possible. (Damber & Aus 2008.) However, following androgen-deprivation therapy, the disease will eventually progress into castration resistance, where the treatment is no longer effective (Nguyen et al. 2014). While there are no curative treatments for CRPC, several new treatment options, such as the anti-androgen enzalutamide and the androgen synthesis inhibitor abiraterone, are available (Scher et al. 2012; De Bono et al. 2011). Also, a novel immunotherapy method, Sipuleucel-T has shown promise in the treatment of CRPC (Kantoff et al. 2010).

2.1.3 Carcinogenesis

Development of prostate cancer is associated with the formation of prostatic intraepithelial neoplasia (PIN) – an abnormal pattern of prostate cells (Bostwick 1989). PIN can be observed within the epithelium as neoplastic changes in the lining of the secretory cells, prostatic ducts, and acini. This includes nuclear and nucleolar enlargements, which are also observed in prostate cancer. In addition, a basal cell layer is still retained with PIN, but is notably absent in prostate cancer. (Montironi et al. 2007.)

PIN can be divided into two distinct grading systems: low-grade PIN and high-grade PIN. Presence of high-grade PIN indicates a significant risk of prostate adenocarsinoma. High-grade PIN is diagnosed with histopathological analysis of a prostate biopsy. (Pacelli & Bostwick 1997.) It is estimated that high-grade PIN can develop into prostatic adenocarcinoma within 10 years (Bostwick et al. 2004). Recently, other morphological changes, such as proliferative inflammatory atropy (PIA), are suggested to have a connection in prostate cancer development to PIN or carcinoma. PIAs are considered to be genetically unstable benign lesions that can develop into PIN or carcinoma. (Woenckhaus & Fenic 2008.)

The initiation of prostate cancer is linked to several molecular level functions, such as inflammation, oxidative/DNA damage, and telomere shortening. Further progression of PIN to adenocarcinoma is linked to oncogene-induced cellular senescence and many molecular mechanisms. (Shen & Abate-Shen 2010.) Cellular senescence is a function of the cell, which prevents unlimited proliferation driven by oncogenes, working as a tumor-suppressor mechanism (Campisi 2001). The common tumor suppressor genes *Pten* and *P53* are both linked to cellular senescence and cancer progression (Chen et al. 2005). The progression into metastatic prostate cancer is largely correlated with the histological grading and aggressiveness of the cancer. However, the concrete metastatic pathways still remain elusive. Most common sites of prostate cancer metastases are lymph nodes, bones, lung, and liver. (Bubendorf et al. 2000.) The key molecular processes and genes behind PCa progression are shown in figure 2.

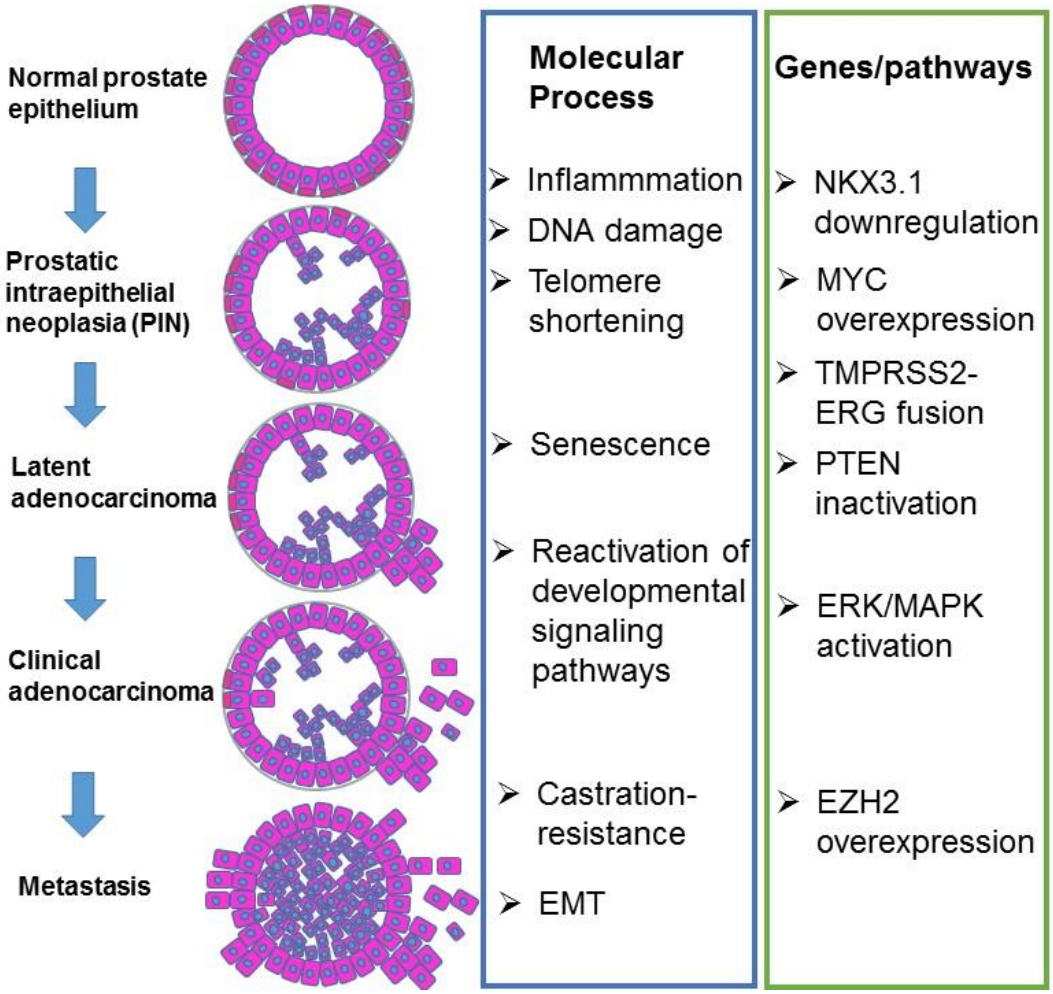

FIGURE 2. The molecular processes and key genes involved in prostate cancer progression from normal epithelium to metastasis

2.2 Prostate cancer biomarkers

2.2.1 MicroRNAs and cancer

Close to 97% of the human genome consists of non-coding DNA. A number of genes in these non-coding areas are responsible for encoding microRNAs. (Lin et al. 2006.) MicroRNAs (miRNAs) are small (20-24 nucleotides) non-coding RNAs that regulate gene expression post-transcriptionally (NCBI Reference Sequence Database 2013). Recently, it has been found that over 60% of protein-coding genes are putative targets of miRNAs in humans (Friedman et al. 2009).

Of the transcription machinery, polymerase II is responsible for miRNA transcription. First, a pri-miRNA is produced by polymerase II. Pri-miRNAs are a group of hairpin-like structures that can be either protein-coding or non-coding. One hairpin structure is chosen by the Drosha ribonuclease III enzyme, which cleaves a 70-nucleotides-long stem-loop precursor miRNA (pre-miRNA) out of the structure. Pre-miRNA is further cleaved by Dicer ribonuclease to generate the miRNA and antisense miRNA star (miRNA*) structures. The miRNA is then linked to a RNA-induced silencing complex (RISC), which can attach to the target mRNA with imperfect base pairing. The binding site to the target mRNA is generally in the 3′ untranslated region (3′UTR). The attachment of a RISC-complex to the mRNA leads either into translational inhibition, or into destabilization of the mRNA, causing a change in gene expression. (NCBI Reference Sequence Database 2013.) A simplified version of miRNA biogenesis is shown in figure 3.

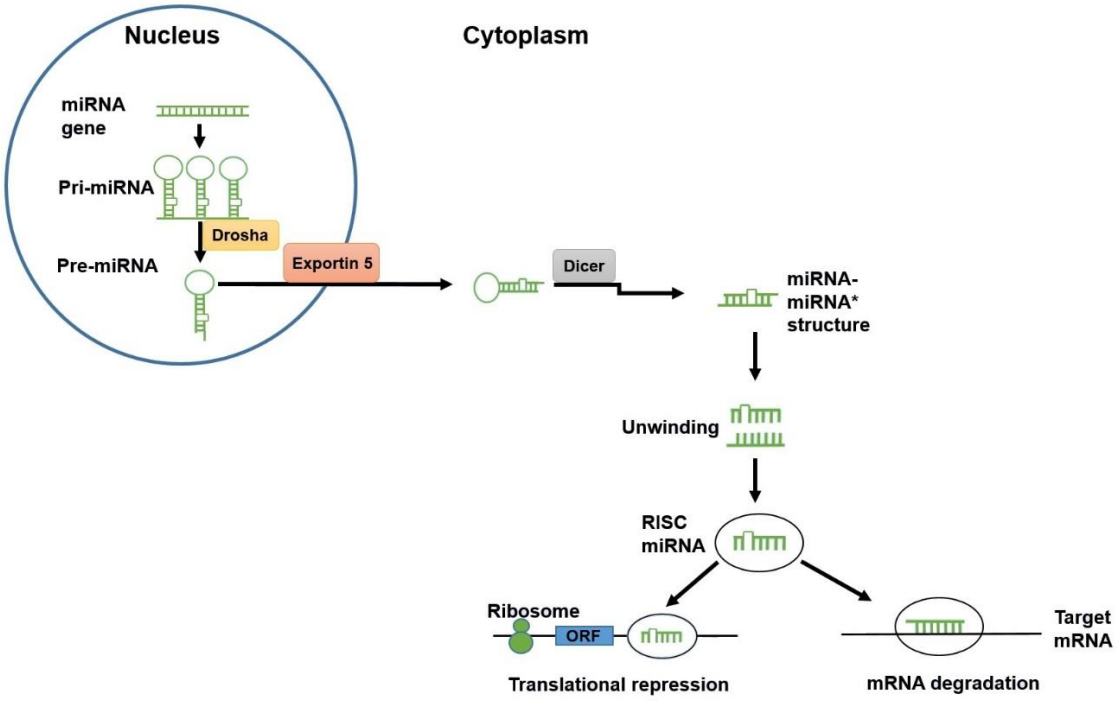

FIGURE 3. A simplified illustration of the miRNA biosynthesis pathway

Recent evidence suggests that some microRNAs have a role in cancer as oncogenes or tumor suppressors. It has been shown that miRNA dysregulation exists in all studied tumor-types, including the prostate. The effect can be similar to dysregulation of oncogenes and tumor suppressor genes. This further highlights the importance of identifying all the targets of miRNAs in cancer, in order to establish their role in cancer carcinogenesis. It has been shown that the dysregulation can be caused by mechanisms such as deletion,

amplification, mutation, epigenetic changes, and other events leading to the formation of cancer. In case the targets of the miRNAs are essential to the survival of the cancer phenotype, downregulation of a gene with a specific miRNA could lead to a potential cure, or to discovery of a biomarker for cancer treatment or detection. (Croce 2009.)

MicroRNA-32 is a miRNA that is located on chromosome 9 (9q31.3) and consists of 22 nucleotides (Fang & Gao 2014). Based on recent evidence, miR-32 was found to be potentially important in the development of castration-resistant prostate cancer. It has also been shown to be androgen-regulated and overexpressed in CRPC. (Waltering et al. 2011; Urbanucci et al. 2012; Jalava et al. 2012.) A link to the reduced expression of B-cell translocation gene 2 (Btg2) – an anti-proliferative protein important for the correct function of the cell – has also been demonstrated in cell cultures. This evidence indicates that miR-32 a potential biomarker and a drug target for prostate cancer. (Jalava et al. 2012.) MicroRNA-32 has also been shown to downregulate the tumor suppressor gene Pten, post-transcriptionally, in cancers such as colorectal carcinoma, and to promote growth, migration, and invasion of the cancer (Wu et al. 2013).

2.2.2 Proliferation marker Ki-67

Ki-67 is a nuclear antigen, which can be used for evaluating cell proliferation. It is found during all phases of the cell cycle, except G_0, making it an excellent marker for cancer. (Van der Kwast 2014.) The forkhead-associated domain (FHA domain) of Ki-67 enables it putatively to interact with phosphorylated proteins, linking it to an important protein network responsible for driving cell division cycles (Li et al. 2004).

Expression of Ki-67 in cancer tissue is called the Ki-67 proliferation score, which can be quantified from immunohistochemically stained tissues. A high Ki-67 score in breast cancer is typically associated with poor prognosis and aggressive disease. (Urruticoechea et al. 2005.) Ki-67 is also one of the most studied biomarkers in prostate cancer. However, its prognostic value in cancer diagnosis still requires further research as prostate cancer is a highly heterogeneous disease. (Fisher et al. 2013.) Ki-67 expression is typically rare in normal prostate tissue where epithelial proliferation is uncommon. However, Ki-67 expression can be seen, for example, in the ventral prostate and dorsolateral prostate in some mouse models. (Stanbrough et al. 2001.)

2.2.3 B-cell translocation gene 2 (*BTG2*)

B-cell translocation gene 2 (BTG2) belongs to a family of antiproliferative proteins called BTG/Tob. Other members of the Btg family include Btg1, tob, tb2, Ana/Btg3, and Pc3k proteins. All of these proteins have similarities in their amino-terminal region with the Btg1 homology domain. BTG/Tob family proteins are all nuclear proteins, responsible for the regulation of several genes. (Kawamura-Tsuzuku et al. 2004.)

Expression of Btg2 has been linked to important cell processes, such as cell cycle progression, differentiation, and apoptosis. It is a primary response gene, which is induced by different growth factors and tumor promoters. Also, Btg2 seems to be responsible for activating mRNA degradation, thus controlling gene expression. (Mauxion et al. 2008.) Based on recent evidence, Btg2 seems to have an important role in preventing carcinogenesis and cancer. In addition, Btg2 has been shown to be an important effector of p53 signaling, which inhibits cellular transformation, suggesting that Btg2 is a tumor suppressor gene. (Boiko et al. 2006.)

According to recent evidence, Btg2 is a target of miR-32 in cell cultures. Btg2 expression is shown to be drastically reduced in CRCP and notably reduced in prostate cancer. There is evidence suggesting that Btg2 is associated with the aggressiveness of the disease, making it a possible biomarker for aggressive prostate cancer. (Jalava et al. 2012.) In addition, Btg2 is shown to be regulated by other miRNAs, such as miR-21 and miR-148a (Jalava et al. 2012; Coppola et al. 2013).

Downregulation of Btg2 is suggested to be linked to the early events of the PCa progression. Loss of Btg2 leads to susceptibility of oxidative DNA damage, as Btg2 is involved in the pathway responsible for DNA damage repair, leading to further cellular damage and progression of the disease. In prostate tissue, Btg2 is mainly localized in the basal cells – the cells mainly responsible for prostatic proliferation. However, in prostatic lesions, Btg2 expression can be detected in most cell types, not just the basal cells. (Ficazzola et al. 2001.)

2.2.4 Tumor suppressor gene *PTEN*

Phosphatase and tensin homolog (*PTEN*) is a tumor suppressor gene, located on chromosome 10 (10q23) (Celebi et al. 2000). In humans, The PTEN protein acts as a lipid phosphatase, responsible for the regulation of phosphatidylinositol 3-kinase (PI3K)/Akt-signaling pathway, modulating cell cycle progression (Kanamori et al. 2001; Ohigashi et al. 2005). Loss of *PTEN* is observed in many primary tumors, including tumors of the prostate, and in up to 60% of metastases, cell lines, and xenografts (Hermans et al. 2004). Recently, it was found that loss of *PTEN* is an early event in the development of prostate cancer. Loss of *PTEN* is also associated with prostate cancer recurrence and poor prognosis. (Yoshimoto et al. 2006; Yoshimoto et al. 2007.)

Several mouse phenotypes can be used to investigate Pten expression. *Pten* knockout mice have been created with the inactivation of *Pten* gene, causing a disease progression similar to humans. (Wang et al. 2003.) Mice with a homozygous deletion of *Pten* ($Pten^{-/-}$ or *Pten* null) aren't viable, making them embryonic lethal (Di Cristofano et al. 1998). *Pten* heterozygous ($Pten^{+/-}$) mice are prone to develop neoplastic lesions in several organs, including the prostate. PIN lesions are mainly detected in the dorsolateral prostate and anterior prostate, but not the ventral prostate. However, even with the development of PIN, $Pten^{+/-}$ mice generally do not progress to adenocarcinoma. (Blando et al. 2009.)

Mice with a prostate-specific homozygous deletion of *Pten*, however, are linked to advanced disease and metastasis. The difference between these phenotypes is seen mainly in the timing of the disease development and progression. A conditional, homozygous deletion of *Pten* can significantly shorten the time required for the formation of PIN from 8–10 months (heterozygous) to 1.5 months (homozygous). In wild type prostates, Pten expression can be seen in the nuclear and cytoplasmic compartments. A low level of expression is also seen in the prostatic epithelial cells and the stromal cells near the prostatic acini. (Wang et al. 2003.)

2.3 Methods for histological analysis

2.3.1 Anatomy and histology of mouse prostate

Human prostate is a distinct, lobular structure, surrounding the urethra. In comparison, the mouse prostate consists of multiple lobes that can be divided into anterior (AP), dorsolateral (DLP), and ventral prostates (VP). Dorsolateral prostate can be further divided into lateral prostate (LP) and dorsal prostate (DP). The lobes are separated by a thin mesothelial-lined capsule. The lobes themselves consist of multiple ducts and tubules, surrounded by a dense fibromuscular stroma. Of all the prostate lobes, dorsolateral prostate is said to resemble the human prostate best. (Shappell et al. 2004.) For histological analysis, the prostates are collected from euthanized mice by following strict guidelines for the welfare and use of animals in cancer research (Workman et al. 2010). Figure 4 illustrates an H&E stained mouse prostate and surrounding structures.

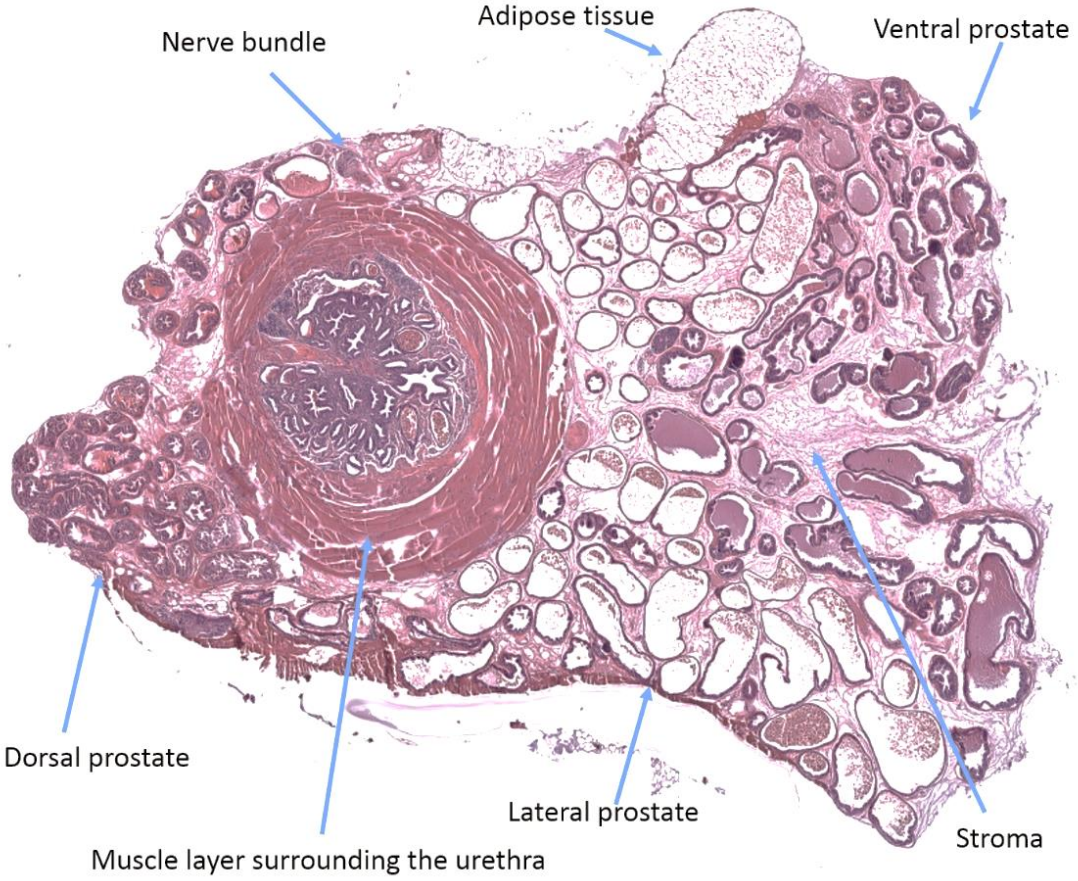

FIGURE 4. H&E stained overview of a PAXgene-fixed paraffin embedded mouse prostate (Image: Leena Latonen, modified)

With histological examination of the anterior prostate (AP), a complex luminal structure can be observed. AP is located in close proximity to the seminal vesicles. Frequent mucosal folding inside the gland is typical. Epithelial cells in the AP grow in a more cubical and columnar shape with central nuclei, and barely visible – or small nucleoli. Eosinophilic granular cytoplasm is also observed. (Shappell et al. 2004.)

The dorsal and lateral prostates are usually combined together as the dorstolateral prostate. However, they are quite distinctive when compared histologically. The mouse dorsal prostate (DP) is typically surrounded by columnar, and stratified or tufting epithelium. The epithelium is usually thinly layered, and no clear mucosal folding is observed. The secretory cells of DP also have a slightly eosinophilic granular cytoplasm, and the gland secretions are homogenous and eosinophilic. Shape of the nuclei and nucleoli is similar to AP. In comparison, the lateral prostate (LP) has more flat, luminal edges, no clear infolding, and a wide luminal space, containing eosinophilic secretions. However, the DP has an increasingly large amount of eosinophilic secretions compared to LP. (Shappell et al. 2004.)

The ventral prostate (VP) has flat, luminal borders, and clear epithelial tufting and infolding. It is typically surrounded by a thin, fibromuscular stroma. The luminal spaces of VP are typically filled with homogenous secretions. The nuclei and nucleoli of VP are also small, uniformed, and located basally. When compared to the DP, the nuclei are typically more centered, and are found in a single-layered shape. (Shappell et al. 2004.)

2.3.2 Tissue preparation in histology

Histological sample preparation can be divided into four basic steps: fixation, processing, embedding, and sectioning. In fixation, a tissue sample is removed from its original *in vivo* environment, and quickly immersed in a fixative, in order to halt natural degeneration of the tissue after death. Tissue degeneration is typically caused by hypoxia, lysosomal enzymes, and putrefactive changes, which all occur in the tissue after death. (Renshaw 2006, 47–48.) Multiple factors, such as hydrogen ion concentration, temperature, penetration, osmolality, concentration, and duration affect the fixation process. In order to retain the original structures, close to neutral pH is needed, as changes in pH may affect

biological systems. Penetration of the fixatives can also affect tissue staining: thin and small tissue samples are necessary for proper diffusion of fixatives. Poor fixation can also be caused by hypertonic solutions, which shrink the tissue – or hypotonic solutions, which cause the tissue to swell. (Hopwood 2002, 69–71.) Especially 10% neutral-buffered formalin is commonly used in histology as a chemical fixative (Sato et al. 2014).

In addition to formalin fixation, other methods, such as PAXgene fixation, have gained popularity recently. PAXgene fixation is an alcohol-based method, where a 2-reagent system prevents cross-linking and degradation of the tissue. According to recent evidence, PAXgene fixation gives comparable results to formalin fixation when used in both *in situ* hybridization and immunohistochemistry. However, in some cases, the results can be better with immunohistochemistry. Slight differences in tissue morphology can be observed when compared to traditional formalin-fixed paraffin embedded (FFPE) tissues. (Kap et al. 2011.)

Fixatives are usually water-based, thus a process is needed where the tissue is dehydrated, in order to allow impregnation of paraffin wax. The aim of dehydration is to remove all residuals of water-soluble fixatives, usually with a raising ethanol gradient. Next, the tissue sample is treated with a clearing agent, such as xylene, toluene, or chloroform. The clearing agent causes the tissue to become translucent, improving the following step of paraffin wax impregnation. Paraffin wax is a mixture of different hydrocarbons with a varying melting point of 40–70 °C. (Anderson & Bancroft 2002, 85–90.) Next, the tissue is embedded in paraffin, cast into a mold of specific size, and promptly cooled on a cold plate. After solidification, the mold is removed and the tissue block is ready for sectioning with a microtome. (Anderson & Bancroft 2002, 89.)

A microtome is an instrument that can be used for sectioning paraffin embedded tissue samples. They can repeatedly cut thin sections of paraffin with a steel knife or a blade. The sections are usually 5–15 μm thick. (Ross & Pawlina 2011, 2.) Several types of microtomes are available, but the most common ones are rotary microtomes and sliding microtomes (Anderson & Bancroft 2002, 86–90). After successful sectioning, the tissue is fixed to a microscope slide in a thermostatically controlled water bath with a temperature of about 10 °C below the melting point of the paraffin wax. The water bath ensures the sections are properly even, thus ensuring a proper morphology for analysis. The use of a proper section adhesive, such as poly-L-lysine or 3-aminopropyltriethoxysilane, is

necessary in order to ensure strong retention of the tissue to the slide. (Anderson & Bancroft 2002, 95–96.) However, there are commercially available products, such as the SuperFrost® Plus slides that require no special adhesives because of their electrostatical coating. After the treatment, the slides are shortly heat-treated in order to allow the surrounding paraffin to melt. Heat-treatment is then followed by different histological staining methods, such as the basic hematoxylin & eosin staining method. (Anderson & Bancroft 2002, 97; Ross & Pawlina 2011, 2.)

2.3.3 Hematoxylin & eosin staining

Hematoxylin & eosin (H&E) staining is by far the most common basic staining method in histology. Hematoxylin is a component that stains the cell nuclei blue/black and gives a good detail of the intra-nuclear space. Eosin is responsible for staining cell cytoplasm and connective tissue fibers in different intensities of pink, orange, and red. (Wilson & Gamble 2002, 125.) However, H&E staining has its faults, as it does not display important structural components, such as elastic material, reticular fibers, certain membranes, and lipids. For staining these components, other methods must be utilized. (Ross & Pawlina 2011, 3.)

A tissue sample, which has been embedded in paraffin, sectioned, placed on a slide and dried in an oven, can be subjected to H&E staining. The slides are immersed in a series of solutions in order to hydrate the tissue. This includes xylene, alcohol, and water. Proper hydration for the slides is essential in order to give the cells affinity for the dyes. The slides are first stained with hematoxylin which stains the nucleus, and next, with eosin which acts as a counterstain. After rinsing in water, the slides are immersed in water, alcohol, and xylene in order to dehydrate the slides. However, if using a water-soluble mounting medium, the previous process can be excluded. Last, a coverslip can be attached to the slides, with the help of a mounting medium, enabling further histological analysis. (Sigma-Aldrich 2002.)

2.3.4 MicroRNA *in situ* hybridization

In situ hybridization is a technique that allows the detection of a specific nucleic acid sequence in its cellular environment. The technique can be utilized on basic formalin-fixed and paraffin embedded (FFPE) samples. The tissue sample is first pre-treated with proteinase-K to unmask the targeted nucleic acid sequence, and then hybridized with a complementary nucleic acid probe. A label is attached to the probe, which makes it possible to visualize the target sequence by light microscopy. (Jones 2002, 555.) MicroRNA *in situ* hybridization (miRNA ISH) is a technique that focuses on the determination of miRNA expression at a cellular level (Nielsen 2012, 67).

Implementation of the miRNA ISH technique has been found to be relatively challenging in a laboratory setting due to the complexity of the process. Typically, ISH protocols use either DNA or RNA probes, depending on the focus of the analysis. However, the probes used in miRNA ISH are LNA:DNA chimeric probes, such as the commercial LNA™ probes, which significantly shorten the process to less than 20 steps. (Nielsen 2012, 67–68.) LNA probes are modified DNA probes that contain locked nucleic acid (LNA) residues – a new class of bicyclic RNA analogs that have a higher-than-normal affinity to their complementary targets. LNA probes increase the thermal stability of the formed hybrids. (Thomsen et al. 2005.)

First, the FFPE slides are deparaffinized in xylene and ethanol solutions in order to remove excess paraffin from the slides. Additionally, other agents, such as hexane, can be used for deparaffinization. Next, nucleic acid sequences are unmasked. As formaldehyde based fixatives mask nucleic acid sequences, the addition of proteinase-K is essential for successful miRNA ISH staining. Proteinase-K digests any nucleases present in the tissue sample, guarding against nucleic acid degradation. It is essential to optimize the proteinase-K concentration in order to have optimal nucleic acid unmasking. (Jones 2002, 564–565.) The slides can then be dehydrated with ethanol to prepare for the hybridization (Nielsen 2012, 72).

Conventional formaldehyde fixation has been shown to cause significant miRNA loss. To prevent the loss of miRNAs from the tissue section, additional fixation with 1-ethyl-3-(3-dimethylaminopropyl) carbodiimide (EDC) can be used. EDC has been shown to

irreversibly fix the miRNA at its 5'phosphate, preventing significant miRNA loss during *in situ* hybridization. (Pena et al. 2009.)

Optimization of the hybridization step is also important. The aim is to avoid non-specific interaction with other nucleic acids, and to maximize the reaction of the probe and the target sequence. First, the target sequence must be rendered single-stranded. The slides are placed in a hybridization chamber with strictly-controlled temperature and time. Usually temperatures of 25°C below the melting point are suitable. Variations in the temperature can influence the success of the annealing process, and lead to poor signal. (Jones 2002, 565–566.) The LNA™ probes are usually double-digoxigenin (DIG) labeled for chromogenic detection by light microscopy (Nielsen 2012, 69).

For reliable results, controls must be used for the miRNA ISH. Typically, a positive control and a control with no hybridization are included. The positive control contains a target sequence that is similar to the target probes. The purpose of the positive control is to verify the overall performance of the used technique and the specificity of the acquired signal. The no-hybridization control lacks a LNA™ probe, thus providing information on any non-specific interaction of other agents used in the analysis. (Jones 2012, 567.) A popular positive control for *in situ* hybridization is the small nuclear RNA (snRNA) U6, localized in the nucleoli. U6 is essential for correct pre-mRNA splicing. (Gerbi & Lange 2002.) Scrambled DNA – a probe without the target sequence – can be used as a negative control, as it only causes non-specific staining (Exiqon 2011, 27).

After the hybridization, the slides are subjected to stringent washing steps, where the hybridization is halted. Proper duration of the washing steps is important, as insufficient washing can cause high background staining. (Exiqon 2011, 28.) After stringent washing steps, the slides are incubated in a blocking solution. The blocking solution is used to reduce non-specific binding of the hybridization probe. Next, alkaline phosphatase-conjugated sheep anti-DIG is added. Anti-DIG-AP binds specifically to the double-DIG-labeled probe. After washes, a substrate solution, such as the nitro blue tetrazolium/5-bromo-4-chloro-3-indolyl phosphate (NBT/BCIP) substrate reagent, is added. Addition of the substrate makes the miRNA expression visible by light microscopy, as a blue end-product is formed. The substrate is sensitive to light during development, so protection from all light sources is necessary. In addition, Nuclear Fast Red counterstain can be added to ease the recognition of surrounding structures near the miRNA expression site.

After washes and a second dehydration, the slides are mounted with a suitable mounting medium, and a coverslip is attached for observation by light microscopy. (Nielsen 2012, 72–73.) Figure 5 summarizes the possible steps of a miRNA ISH technique. Washes with PBS are not shown in the figure, as they are mandatory after each step.

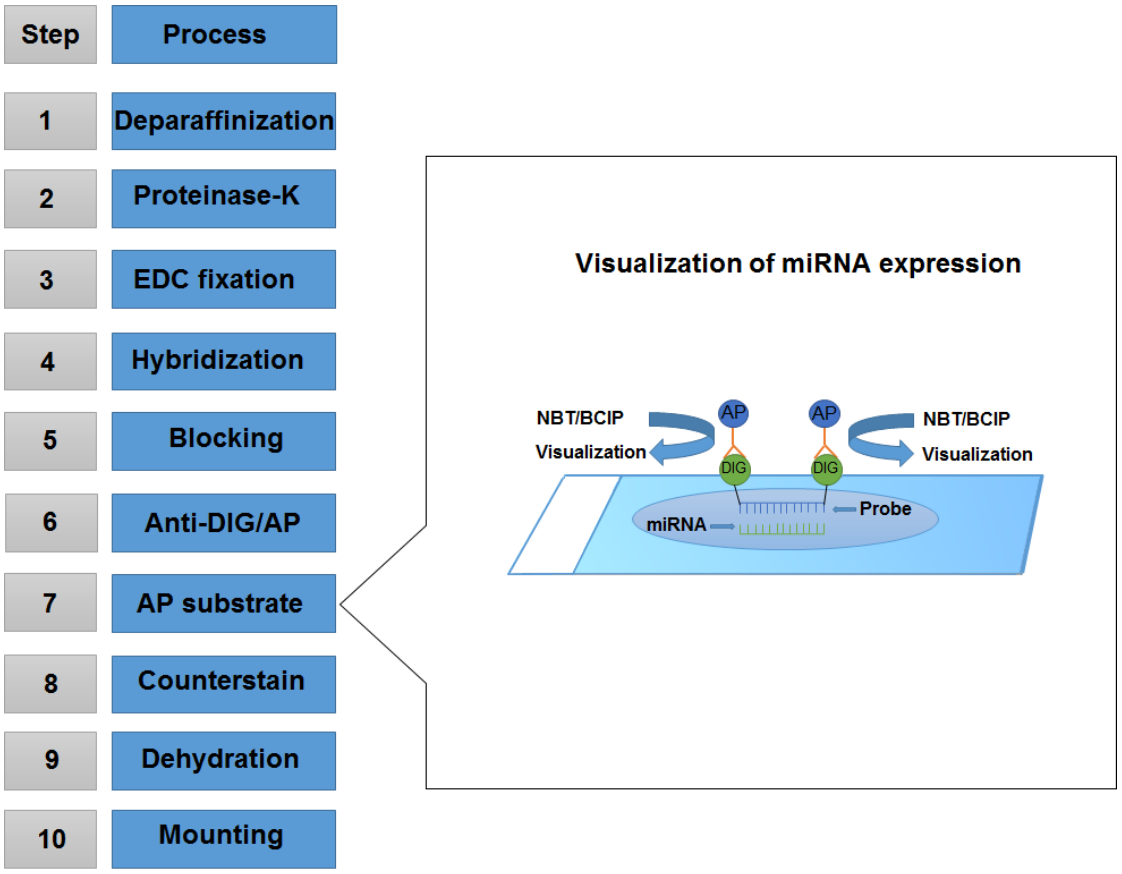

FIGURE 5. Typical steps in a miRNA ISH protocol

2.3.5 Immunohistochemistry

Immunohistochemistry (IHC) is a technique for visualizing the specific immunologic reaction of an antigen and an antibody. It can be utilized, in addition to research purposes, in the diagnostics of clinical pathology. Typical uses of IHC include phenotyping, examination of morphology, and clinical diagnoses. It is especially important for studying the location of different biomarkers in tissues, for example in cancer research. (Miller 2002, 421–423.)

Antibodies are a group of proteins called immunoglobulins (Ig). Immunoglobulins are found in plasma or serum, and they are divided into 5 major categories: IgG, IgA, IgM,

IgD, and IgE. They are formed by the immune system after B lymphocytes recognize foreign antigens and transform into plasma cells. Immunoglubulins IgG and IgM are the most frequently used antibodies in immunohistochemistry. Immunoglobulins have a common structure: they are formed by two light and heavy polypeptide chains, linked together with disulfide bonds. The terminal regions in these molecules have varying amino acid sequences, also known as variable domains. These variable domains are the reason antibodies can bind to specific antigens, as certain amino acid sequences bind specifically on epitopes of the antigens. Epitopes, or antigenic determinant groups, are a small group of amino acids or monosaccharide units that are found on the topographical regions of the antigens. Antigens themselves can be either proteins, carbohydrates, or lipid molecules. (Miller 2002, 423–424.)

Antibodies can be produced either as poly- or monoclonal. Polyclonal antibodies are produced in animals that are immunized with a specific molecule – an immunogen – containing the desired antigen. As a result, the immune system of the animal produces antibodies to counter the foreign antigens. The antibodies can be harvested by bleeding the animal and collecting the serum. The plasma cells of the animal produce antibodies that have a slightly different affinity towards other epitopes of the immunogen, making the antibodies polyclonal. Due to the polyclonal nature of the antibodies, there can be significant variability in different batches when compared to monoclonal antibodies. (Miller 2002, 424.)

Monoclonal antibodies, unlike polyclonal antibodies, are produced in a single cell line using hybridoma cell lines. The technique takes advantage of plasma cells for the production of specific antibodies, and the immortality of a neoplastic myeloma cell line. These functions are combined to produce a hybridoma which has the combined abilities of both cell types. Due to the limitless growth of the hybridoma cell line, the cells can be cloned and grown in cell culture in almost unlimited numbers. With common screening techniques, the antibodies can be produced without the cross-reactivity that can be found in polyclonal antibodies. The hybridoma cell lines will produce pure, specific antibodies in a constant supply, which can be especially useful in immunohistochemistry. (Miller 2002, 424.)

To visualize the binding of an antibody and an antigen, a label must be used. Especially enzymes are widely used in immunohistochemistry. When enzymes are incubated with a

chromogen, a colored end-product is produced that can be visualized by light microscopy. Horseradis peroxidase (HRP) and calf intestinal alkaline phosphatase (AP) are widely used. When HRP is combined with 3,3´-diaminobenzine tetrahydrochloride (DAB), a stable, dark brown end-product is formed. (Miller 2002, 424–425.) Alkaline phosphatase, on the other hand, produces an insoluble black-purple end-product when incubated with a combination of nitro-blue tetrazolium chloride (NBT) and 5-bromo-4-chloro-3'-indolyphosphate p-toluidine salt (BCIP) (Thermo Scientific 2014).

Conjugation of a label to an antibody can be performed with two distinct techniques: traditional direct technique and indirect technique. In the direct technique, the primary antibody is conjugated directly to the label. Utilization of the direct technique is relatively simple, as only one application of an antibody is needed, along with the substrate solution. In the indirect technique, an unconjugated primary antibody is applied first, followed by a labeled, secondary antibody. Application of a secondary antibody increases signal sensitivity due to increased interactions between the two antibodies, increasing the amount of substrate attached to the sample. (Miller 2002, 426–427.)

In addition to basic methods, several other modified techniques with significantly higher sensitivity are available. For example, the avidin–biotin technique (ABT) has been found to have high sensitivity. This technique relies on the high affinity of the glycoprotein avidin for biotin. Multiple biotin molecules can be attached to a single antibody, followed by the conjugation of a labeled avidin, leading to a heightened signal. (Miller 2002, 427.)

Recently, more advanced commercial techniques have surfaced as well. For example, certain polymer-based techniques, such as the EnVision™ FLEX+ system (Dako) or the N-Histofine® Simple Stain MAX PO (multi) detection reagent (Nichirei Biosciences), offer a universal reagent that can be used to detect almost any tissue-bound primary antibody, regardless of the origin (rabbit or mouse). Both of these methods consist of a polymer backbone, on which the antibodies and enzymes can attach to. (Key 2009, 58–59.)

Samples in immunohistochemistry are typically either frozen sections or FFPE sections. After proper fixation and sample preparation, the samples are first subjected to deparaffinization with solvents, such as xylene or n-hexane. Excess traces of the solvents are then removed by rehydrating the sample with ethanol. As tissue fixation and processing may change the structure of the antigen epitopes, the samples are subjected to antigen

retrieval techniques, where the original antigen epitopes are restored. This can be achieved with different proteolytic enzymes, heat-mediated techniques or a combination of these methods. (Miller 2002, 435–440.)

Traditional formalin fixation alters the three-dimensional structure of several tissue proteins, thus making the demasking of epitopes important for a successful IHC staining. Heat-induced epitope retrieval (HIER) is a commonly used method for the demasking of epitopes. HIER can be achieved with many techniques, such as the conventional water bath heating, pressure cooker heating or microwave oven heating. For example with water bath heating, the sample slides are first placed in a buffer (citrate buffer pH 6 or Tris-EDTA buffer pH 9), which is then heated to around + 97 °C for 20 minutes. After cooling, the samples can be directly subjected to immunohistochemical staining. (Kumar & Rudbeck 2009, 51–52.)

Next, the samples are subjected to a blocking technique, where unspecific background staining is prevented. Blocking is usually performed with a buffer containing an immunoglobulin that does not interact with the primary antiserum. The blocking agent is produced in the same species as the primary antibody. Background staining is typically caused by hydrophobic and electrostatic forces in certain locations of tissues. (Miller 2002, 435–440.)

After successful blocking, IHC staining can be performed. For example, in the avidin–biotin technique, samples are first incubated in a primary antibody, followed by a biotinylated secondary antibody. Next, a streptavidin-enzyme conjugate can be used, followed by a substrate-chromogen mixture. All steps in the staining process are followed by washes in order to remove trace amounts of the previous solution. (Thermo Scientific 2014.) After staining, the slides are typically counterstained with hematoxylin to improve morphological recognition. Counterstaining is followed by dehydration with ethanol, followed by a clearing agent, and finally, with the addition of a coverslip with a proper mounting reagent. (Miller 2002, 453–454.) Figure 6 summarizes a simplified version of a standard immunohistochemical staining process.

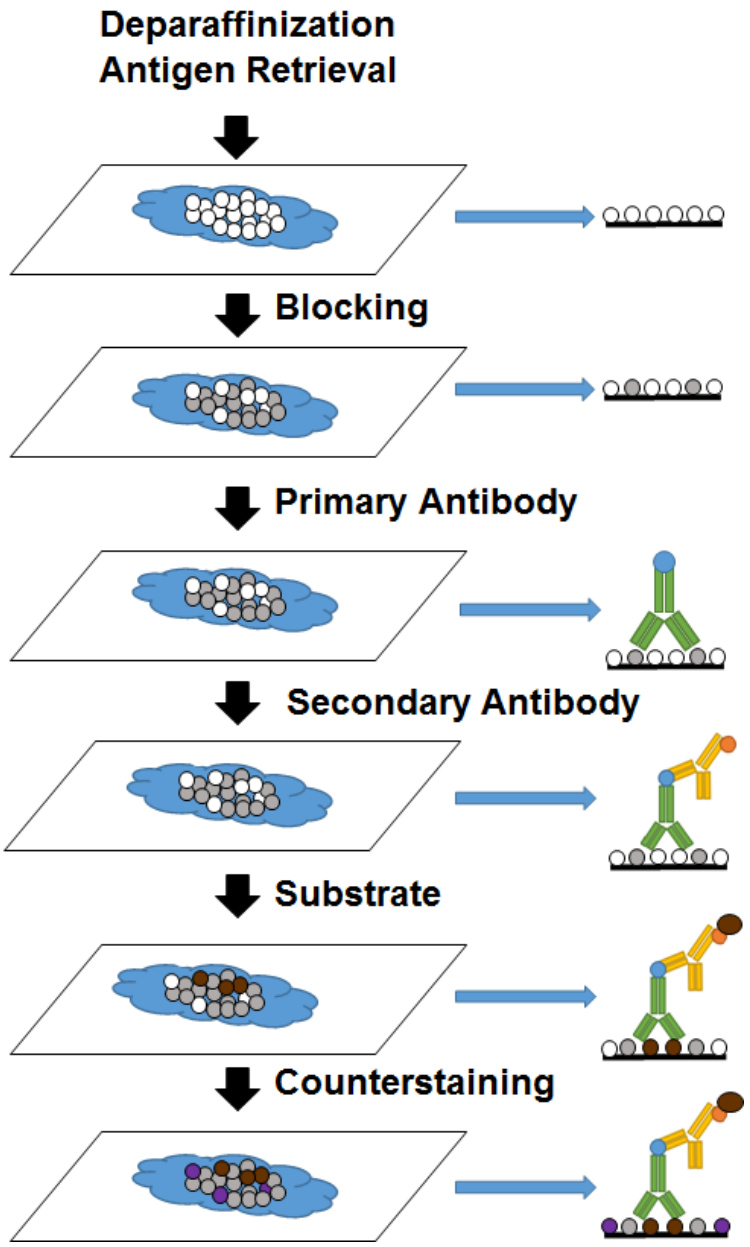

FIGURE 6. A simplified version of the steps in a standard IHC staining process

3 AIM OF THE STUDY

The objective of the thesis is to study the expression of several putative biomarkers in transgenic mouse prostate tissue. This thesis will help improve further histopathological examination of prostate cancer for the Molecular Biology of Prostate Cancer group in hopes of finding putative biomarkers and treatment options for prostate cancer (PCa) and castration-resistant prostate cancer (CRPC).

The purpose of the thesis is to establish protocols for the *in situ* hybridization of miR-32 and the immunohistochemistry of Ki-67, Btg2, and Pten – and to study the expression of these putative biomarkers in PAXgene-fixed paraffin embedded (PFPE) or formalin-fixed paraffin embedded (FFPE) mouse prostate tissue. The establishment of the *in situ* hybridization protocol for miR-32 will help evaluate the success of the transgenic mouse line, previously established by the research group, expressing miR-32 specifically in the prostate. By establishing protocols for the immunohistochemistry of Ki-67, Btg2, and Pten, it is possible to investigate the expression of these genes in mouse lines with confirmed prostatic lesions in order to further evaluate their role in prostate carcinogenesis, and in the formation of castration resistance.

4 MATERIALS AND METHODS

4.1 *In situ* hybridization of miR-32

4.1.1 Sample preparation

For *in situ* hybridization, suitable mouse prostate tissue samples were chosen. Both formalin-fixed paraffin embedded (FFPE) samples and PAXgene-fixed paraffin embedded (PFPE) samples were tested. The prostates were obtained, before the project, from mice by separating the prostate, seminal vesicles, and the bladder from the surrounding tissues. The obtained prostates were stored in a container with 10% formalin or the commercial PAXgene fixative. After fixation, the tissue samples were prepared for processing and embedding. Shandon Citadel 2000 Tissue Processor was used for automated tissue processing. The protocol for both FFPE and PFPE processing is shown in table 1.

TABLE 1. The protocol for FFPE and PFPE sample fixation

Step	Substance	Duration
1	Formalin/PAXgene	-
2	70% EtOH	2 h
3	96% EtOH	1.5 h
4	96% EtOH	1 h
5	Abs. EtOH	1.5 h
6	Abs. EtOH	1.5 h
7	Abs. EtOH	1.5 h
8	Xylene	1.5 h
9	Xylene	1.5 h
10	Xylene	1.5 h
11	Paraffin (58 °C)	1.5 h
12	Paraffin (58 °C)	1.5–4 h

Processed tissue samples were then embedded in paraffin. Sakura Tissue-Tek TEC embedding center was used for tissue embedding. The prostate sample was first placed in a Tissue-Tek® mold system in a fixed orientation. 60 °C paraffin was poured in the mold which was placed on a cold plate for a few seconds. A Tissue-Tek® cassette was placed on top of the tissue and paraffin was added until the mold was completely immersed. The

mold was then placed on a cold plate until the paraffin wax solidified. The tissue blocks were stored at room temperature until sectioning.

Both FFPE and PFPE tissue blocks were placed on a + 4 °C cold plate for 15 minutes before sectioning. All surfaces were wiped with RNaseZAP™ solution to remove possible RNAse contaminations. Dry-heat treated glass equipment and DEPC-treated water were used. Leica SM2010 R microtome was used to cut suitable sections from the tissue blocks. S35 disposable microtome blades were utilized to cut 8 – 10 µm thick sections from both FFPE and PFPE samples. The sections were first placed in DEPC-treated water at room temperature, and then attached to SuperFrost™ Plus microscope slides. Next, the slides were placed shortly in + 52 °C water bath to straighten the tissue section. After 30 minutes of drying at room temperature, the samples were placed in an oven at + 62 °C for 45 minutes. After the heat treatment, the slides were stored at + 4 °C overnight for *in situ* hybridization.

4.1.2 Establishment of *in situ* hybridization protocol

A total of 6 samples were used for the protocol establishment. The samples were either PAXgene- or formalin-fixed. Wild type prostates were used. During the establishment, only U6 and Scrambled DNA probes were used, as suitable conditions for the protocol had to be established first. In addition, one PAXgene-fixed sample and one formalin-fixed sample was subjected to H&E staining for better morphological examination.

The previously prepared tissue sections were brought to room temperature from the + 4 °C cold room. First, deparaffinization was performed in order to remove excess paraffin around the tissue. Coplin jars, sterilized with dry-heat (180 °C), were used throughout the entire process. All surfaces, during *in situ* hybridization, were first treated with RNAseZap™ solution to remove possible RNAse contaminations. The slides were immersed in n-hexane, 100% ethanol, and 1X phosphate-buffered saline (PBS), sequentially, by placing them in Coplin jars for indicated times (table 2).

TABLE 2. The protocol for deparaffinization

Step	Reagent	Duration
1	n-hexane	4 min
2	n-hexane	4 min
3	100% EtOH	2 min
4	1X PBS	5 min
5	1X PBS	5 min

After deparaffinization, the slides were prepared for deproteinization. 2.5 µg/ml of proteinase-K in proteinase-K buffer was used. Proteinase-K demasks the microRNAs found in the tissue sample by digesting proteins and contaminations, allowing the probe to hybridize with the target microRNA sequence (Exiqon 2011, 10). The slides were incubated in 300 µl of proteinase-K and immersed, sequentially, in PBS, 4% paraformaldehyde (PFA), 0.2% glycine and last, in PBS (table 3). The exact content of the proteinase-K buffer, 4% paraformaldehyde, and 0.2% glycine is listed in appendix 1.

TABLE 3. The protocol for deproteinization

Step	Reagent	Duration
1	Proteinase-K	20 min
2	1X PBS	5 min
3	1X PBS	5 min
4	4% PFA	10 min
5	0.2% glycine	5 min
6	1X PBS	5 min
7	1X PBS	5 min

After washes with PBS, the slides were incubated in 75 ml of freshly prepared imidazole buffer. The tissues were then circled with a PAP pen, which creates a hydrophobic coating around the tissue, improving the retention of liquid near the tissue. At this point, a additional fixation with EDC was possible. However, during the protocol establishment, EDC fixation was not attempted. The slides were washed with glycine and PBS, respectively. Table 4 shows the duration of the incubations and the concentrations. The exact content of both imidazole buffer and EDC solution is listed in appendix 1.

TABLE 4. The protocol for EDC fixation

Step	Reagent	Duration
1	Imidazole buffer	10 min
2	Imidazole buffer	10 min
3	EDC solution	60 min
4	0.2% glycine	5 min
5	1X PBS	5 min
6	1X PBS	5 min

Next, hybridization was performed. 5'-DIG-labeled U6 LNA™ probe (5'-CACGAATTT-GCGTGTCATCCTT-3') from Exiqon was used as a positive control. 5'-3'-DIG-labeled scrambled DNA LNA™ probe (5'- GTGTAACACGTCTATACGCCCA-3') from Exiqon was used as a negative control. 500 µl of prehybridization buffer was added to each slide at room temperature for 15 minutes. Probes were then denatured at + 90 °C for 4 minutes. 1:50 dilutions were prepared of each probe by diluting with the hybridization buffer. 200 ul of hybridization mix was added on each slide, and the slides were covered with a piece of parafilm, wiped with the RNAseZap™ solution. The slides were then placed in StatSpin® ThermoBrite Denaturation and Hybridization System for 21 hours at the chosen temperature (+ 37 °C). The exact details of both U6 and Scrambled DNA probes, prehybridization buffer, and hybridization buffer is listed in appendix 1.

The next morning, the slides were subjected to stringent washes at the hybridization temperature (+ 37 °C). The slides were immersed in a mix of saline-sodium citrate (SSC) and formamide in Coplin jars. The Coplin jars were placed in a water bath, which was heated to + 37 °C. The slides were rinsed in 0.2X SSC at room temperature to remove trace amounts of formamide, and washed with 1X PBS 0.1% Tween-20. The concentrations and duration of the washes are listed in table 5. The exact details of all the stringent wash buffers is listed in appendix 1.

TABLE 5. The protocol for the stringent washes

Step	Reagent	Duration
1	1st Stringent wash buffer	15 min
2	2nd Stringent wash buffer	30 min
3	3rd Stringent wash buffer	45 min
4	0.2X SSC	5 min
5	1X PBS, 0.1% Tween-20	1 min

After the stringent washes, the slides were placed in Shandon Slide Racks for the staining process. The staining process consisted of multiple phases: incubation in anti-DIG-HRP (1:800 dilution), DIG amplification working solution (1:50 dilution), anti-DIG-AP (1:800 dilution), NBT/BCIP substrate solution (1:50 dilution), and KTBT buffer. Incubations were performed with 200 µl of each reagent. Washes in between the staining steps were performed using 1X PBS 0.1% Tween-20. The incubation with NBT/BCIP substrate was performed at + 30 °C, protected from all light sources. The other staining reagents were added, and washing steps were performed at room temperature. Table 6 illustrates the used solutions and the duration of the incubation periods during the staining process. The exact content of anti-DIG-HRP, DIG amplification working solution, anti-DIG-AP, NBT/BCIP substrate solution, and KTBT buffer is listed in appendix 1.

TABLE 6. The protocol for the staining process

Step	Reagent	Duration
1	1X blocking solution	15 min
2	Anti-DIG-HRP 1:800	30 min
3	1X PBS, 0.1% Tween-20	3X 5 min
4	DIG Amplification solution 1:50	10 min
5	1X PBS, 0.1% Tween-20	3X 5 min
6	Anti-DIG-AP 1:800	60 min
7	1X PBS, 0.1% Tween-20	3X 3 min
8	NBT/BCIP substrate	2 h
9	KTBT buffer	2X 5 min
10	DEPC-treated water	1 min

Next, the slides were subjected to dehydration and mounting. The slides were briefly immersed in an ascending ethanol gradient. After air-drying, 3 drops of Eukitt® quick-hardening mounting medium was added, and a coverslip was attached to the slide. The slides were then left at room temperature, and subjected to analysis by light microscopy the following morning. The exact process of dehydration is listed in table 7.

TABLE 7. The protocol for dehydration

Step	Reagent	Duration/immersion
1	70% EtOH	10 times
2	70% EtOH	1 min
3	96% EtOH	10 times
4	96% EtOH	1 min
5	100% EtOH	10 times
6	100% EtOH	1 min

4.1.3 *In situ* hybridization of miR-32 and protocol optimization

The *in situ* hybridization of miR-32 was performed by following the previously established protocol – with only minor modifications along the way. A total of 24 samples in three separate attempts were subjected to *in situ* hybridization during the optimization. Only PAXgene-fixed samples were used, as the expression of the test probes was deemed better on the PAXgene-fixed samples compared to formalin-fixed samples. U6 probes and scrambled DNA probes were used during all attempts in order to ensure the specificity of miR-32 expression. Conditions, such as the proteinase-K concentration, probe dilution ratio, EDC fixation, and sample thickness were adjusted during the project. The samples subjected to *in situ* hybridization are listed in table 8.

TABLE 8. The samples used during the optimization of *in situ* hybridization

Samples	Type	Fixation	Probe/process
3	Wild type	PAXgene	U6
3	Wild type	PAXgene	Scrambled DNA
3	Wild type	PAXgene	miR-32
3	Wild type	PAXgene	H&E staining
3	Transgenic	PAXgene	U6
3	Transgenic	PAXgene	Scrambled DNA
3	Transgenic	PAXgene	miR-32
3	Transgenic	PAXgene	H&E staining

5'-3'-DIG-labeled miR-32 LNA™ detection probe (5'-GCAACTTAGTAATGTG-CAATA-3') by Exiqon was used as the sample probe for miR-32 detection. The U6 and Scrambled DNA probes remained the same as in the protocol establishment. Proteinase-K concentration varied between 2.5–10 µg/ml during all the attempts. Probe dilutions of either 1:500 or 1:1000 were used. The hybridization time varied between 16 to 21 hours. However, the hybridization temperature (+ 37 °C) remained the same throughout the optimization attempts. An additional 60-minute EDC fixation was attempted twice during the optimization. Thickness of the tissue samples varied from 8 µm to 10 µm. In addition to *in situ* hybridization, a total of six samples were subjected to H&E staining for better morphological examination, as the *in situ* hybridization samples were not counterstained.

4.1.4 Hematoxylin & eosin staining

In addition to *in situ* hybridization, one slide of each type was subjected to H&E staining. As counterstaining was not used during in situ hybridization, additional H&E staining was required for proper morphological analysis. The H&E stained sample was obtained from the same tissue block as the miR-32 sample, allowing almost identical morphological comparison. After the 45-minute heat treatment, the slides were subjected to H&E staining. Sakura DRS-60 Autostainer was used to automate the staining process. The program for automated H&E staining is listed in table 9.

TABLE 9. The program for the automated H&E staining process

Step	Solution	Time
1	n-hexane	3 min
2	n-hexane	3 min
3	Abs. EtOH	2 min
4	Abs. EtOH	1 min
5	96% EtOH	2 min
6	70% EtOH	1 min
7	dH_2O	30 s
8	Harris Hematoxylin 1:4	4 min
9	H_2O	7 min
10	dH_2O	40 s
11	0.2% Eosin	2 min
12	H_2O	1 min
13	dH_2O	30 s
14	96% EtOH	2 min
15	96% EtOH	2 min
16	Abs. EtOH	1 min
17	Abs. EtOH	2 min
18	Abs. EtOH	2 min

After successful staining, the slides were immersed twice in xylene for 4 minutes. Next, Dako Coverslipper was used to automatically attach a coverslip to each microscope slide. DPX mounting medium (Sigma-Aldrich) was used to attach the coverslip. The slides were left at room temperature overnight until the mounting medium had solidified. The H&E stained slides were then subjected to morphological analysis, along with the samples from *in situ* hybridization, by light microscopy.

4.2 Immunohistochemistry of Ki-67, Btg2, and Pten

4.2.1 Sample preparation

For immunohistochemical staining, both PFPE and FFPE samples were used. The tissue processing and embedding were identical to *in situ* hybridization (table 1). The tissue blocks were first placed on a + 4 °C cold plate for 15 minutes before sectioning. S35 disposable microtome blades were utilized to cut 5–8 µm thick sections. The sections were placed in a water bath at room temperature, attached to SuperFrost™ Plus microscope slides, and placed shortly in + 52 °C water bath to straighten the tissue section. The slides were left at room temperature in an upwards position for 30–60 min to remove excess water. The slides were then placed in an oven at + 62 °C for either 2 hours or overnight. After the heat-treatment, the slides were ready for IHC staining.

4.2.2 Establishment of IHC staining methods

The first task of the immunohistochemical staining was to establish suitable conditions for the staining process. Several key conditions, such as the antibody dilution ratio and the type of the antibody were adjusted during the project. The IHC methods were established for Ki-67, Btg2, and Pten. Most of the conditions remained the same throughout the testing of all three antibodies. A total of 20 samples were used for the method establishment: ten for Ki-67, five for Btg2 and five for Pten.

The heat-treated slides were first subjected to deparaffinization. The slides were immersed in n-hexane twice for 4 minutes and once in 100% ethanol for 2 minutes. After air-drying, the slides were subjected to heat-induced epitope retrieval (HIER). Lab Vision™ PT Module was used to automate the retrieval process. Tris-EDTA buffer solution (TE buffer) pH 9.0, containing 0.05% Tween-20 was first pre-heated to + 65 °C, and the previously deparaffinizated slides were placed in the buffer. The buffer was then heated to + 98 °C for 15 minutes. After cooling, the slides were placed in 1X TBS-Tween-20 until staining. LabVision Autostainer 480 was used to automate the IHC process. Table 10 details the program used for the staining process.

TABLE 10. The IHC staining program for LabVision Autostainer 480

Step	Solution/reagent	Duration
1	TBS Tween	Wash
2	Endogenous peroxidase blocking with 3% H_2O_2	5 min
3	TBS Tween	Wash
4	Primary antibody	30 min
5	TBS Tween	Wash 2x
6	Histofine Simple Stain MAX PO	30 min
7	TBS Tween	Wash
8	TBS Tween	Wash
9	ImmPACT DAB	5 min
10	TBS Tween	Wash 2x
11	TBS Tween	Wash
12	Mayer's Hematoxylin	2 min
13	TBS Tween	Wash

For the IHC staining of Ki-67, two different antibodies were tested: mouse (MM1) anti-Ki67 (Leica Biosystems) and rabbit (SP6) anti-Ki67 (Thermo Scientific). The immunohistochemical staining of Pten was performed with anti-Pten (Cell Signaling Technology) and Btg2 with anti-Btg2 (Santa Cruz Biotechnology). Dilution ratios of 100, 200, 500, 800, and 1000 were tested during the project. Antibody dilutions were made in Normal Antibody Diluent (Immunologic). All samples were cut from PFPE blocks (wild type). Secondary antibody labeling was performed with N-Histofine® Simple Stain MAX PO (multi) detection reagent (anti-mouse and anti-rabbit), developed by Nichirei Biosciences. ImmPACT DAB Peroxidase (HRP) Substrate (Vector Laboratories) was used as the reaction substrate. The samples used for testing are listed in table 11. Exact detail of each antibody and reagent is listed in appendix 2.

TABLE 11. The samples for IHC dilution testing

Sample	Antibody	Dilution
Ki67-350wt-1	Ki-67 (MM1)	1:200
Ki67-350wt-2	Ki-67 (MM1)	1:400
Ki67-350wt-3	Ki-67 (MM1)	1:600
Ki67-350wt-4	Ki-67 (MM1)	1:800
Ki67-350wt-5	Ki-67 (MM1)	1:1000
Ki67-350wt-6	Ki-67 (SP6)	1:100
Ki67-350wt-7	Ki-67 (SP6)	1:200
Ki67-350wt-8	Ki-67 (SP6)	1:500
Ki67-350wt-9	Ki-67 (SP6)	1:800
Ki67-350wt-10	Ki-67 (SP6)	1:1000
Btg2-350wt-1	Btg2	1:100
Btg2-350wt-2	Btg2	1:200
Btg2-350wt-3	Btg2	1:500
Btg2-350wt-4	Btg2	1:800
Btg2-350wt-5	Btg2	1:1000
Pten-350wt-1	Pten	1:100
Pten-350wt-2	Pten	1:200
Pten-350wt-3	Pten	1:500
Pten-350wt-4	Pten	1:800
Pten-350wt-5	Pten	1:1000

After the run, the slides were placed in milliQ water. Dehydration was performed by immersion in 70%, 96%, and 100% ethanol. The exact process is detailed in table 12. After dehydration, the slides were placed in xylene twice for 4 minutes. Dako Coverslipper was used to attach a coverslip on the slides. DPX mounting medium (Sigma-Aldrich) was used as a hardening agent. The slides were left to dry at room temperature until analysis by light microscopy.

TABLE 12. The dehydration process for Ki67, Btg2, and Pten

Step	Reagent	Duration/Immersion
1	70% EtOH	10x
2	70% EtOH	1 min
3	96% EtOH	10x
4	96% EtOH	1 min
5	100% EtOH	10x
6	100% EtOH	5 min

4.2.3 IHC staining of Ki-67, Btg2, and Pten

A total of 14 samples were subjected to immunohistochemistry during the project: four samples for Ki-67, four for Btg2 and six for Pten. IHC staining was performed for both PFPE and FFPE samples. Both wild type (WT) and transgenic (TG) mouse tissue blocks were used for comparison. The samples were chosen from tissue blocks with close morphological similarity to the miRNA ISH samples. For PAXgene-fixed samples of Pten, both homozygous (*Pten*$^{+/+}$) and heterozygous (*Pten*$^{+/-}$) mouse lines were analyzed. The exact details of the samples are listed in table 13.

TABLE 13. The IHC stained samples for Ki-67, Btg2, and Pten

Sample	Type	Fixation	Dilution
Ki67-1	Wild type	PAXgene	1:100
Ki67-2	Transgenic	PAXgene	1:100
Ki67-3	Wild type	Formalin	1:100
Ki67-4	Transgenic	Formalin	1:100
Btg2-1	Wild type	PAXgene	1:800
Btg2-2	Transgenic	PAXgene	1:800
Btg2-3	Wild type	Formalin	1:800
Btg2-4	Transgenic	Formalin	1:800
Pten-1	Wild type/homozygote	PAXgene	1:200
Pten-2	Transgenic/homozygote	PAXgene	1:200
Pten-3	Wild type/heterozygote	PAXgene	1:200
Pten-4	Transgenic/heterozygote	PAXgene	1:200
Pten-5	Wild type	Formalin	1:200
Pten-6	Transgenic	Formalin	1:200

Suitable dilution ratios were determined during the establishment of the protocol. 1:100 dilution was used for Ki-67, 1:800 dilution for Btg2, and 1:200 dilution for Pten. Antigen retrieval was performed with the HIER method, as established previously, by using Tris-EDTA buffer 0.05% Tween-20 (pH 9). Rabbit (SP6) anti-Ki67 was used for the IHC of Ki-67, anti-Pten (Cell Signaling Technology) for Pten and anti-Btg2 (Santa Cruz Biotechnology) for Btg2. The same secondary antibody (N-Histofine® Simple Stain MAX PO) and chromogen (ImmPACT DAB) were used for visualization. The IHC staining was performed with LabVision Autostainer 480 using the same program as listed in table 10.

5 RESULTS

5.1 *In situ* hybridization of miR-32

5.1.1 Established conditions for the *in situ* hybridization

The conditions for *in situ* hybridization were established with four separate attempts. The aim of the project was to establish a working method where the level of expression of miR-32 was sufficient for analysis – not to obtain the absolute optimal conditions. Perfect optimization of the method would have taken much longer than the time allotted for the project.

At first, both FFPE and PFPE tissue samples were used. However, it was quickly noted that the expression of U6 (positive control) in PAXgene-fixed tissues was sufficient for analysis, thus making the inclusion of formalin-fixed samples unnecessary. The hybridization temperature of + 37 °C for 21 hours was found to be suitable. Proteinase-K concentration was found to be suitable for both U6 and miR-32 probes at 5.0 µg/ml. Probe dilution of 1:500, anti-DIG-AP of 1:800, anti-DIG-HRP of 1:800, NBT/BCIP substrate of 1:50 and DIG Amplification working solution of 1:50 were all found sufficient. EDC fixation was found to cause too much background staining, making it difficult to judge specificity. Sample thickness of 8 µm was used to obtain the best results. Sections with the thickness of 10 µm were found to have poor constancy with the staining: not all parts of the tissue were stained evenly. Table 14 illustrates the conditions that were used to obtain successful miR-32 expression. The exact list of reagents used for positive miR-32 expression is listed in appendix 1.

TABLE 14. The conditions for the best miR-32 expression with *in situ* hybridization

Condition	Details
Hybridization temperature	21 h at + 37 °C
Proteinase-K concentration	5.0 µg/ml
Probe dilution	1:500
anti-DIG-AP dilution	1:800
anti-DIG-HRP dilution	1:800
NBT/BCIP substrate dilution	1:50
DIG Amplification working solution	1:50
EDC fixation	No
Sample thickness	8 µm

5.1.2 Expression of miR-32 in transgenic mouse prostate tissue

To investigate the expression of miR-32 in transgenic mouse prostate tissue, the results of *in situ* hybridization of both wild type (WT) and transgenic (TG) prostates were compared. The obtained results are shown in figure 7 as a 40X magnification of the dorsolateral prostate. The pictures were taken manually with the Olympus U-CMAD-2 camera system. Figures 7A–7D represent the staining of WT prostate and figures 7E–7H the TG prostate.

Basic H&E staining of both WT and TG prostates is shown in figure 7A and 7E, respectively, where morphology of the dorsolateral prostate can be seen. As seen in figure 7B and 7F, scrambled DNA probe shows minimal or no expression in both WT and TG prostates. However, some unspecific staining can observed in the WT prostate. Intense U6 expression can be observed in both WT and TG prostates, as seen in figures 7C and 7G. However, significant background staining can also be detected, especially in the TG prostate. A low level of miR-32 expression can be clearly seen (figures 7D and 7H) in both WT and TG prostates when compared to the negative controls.

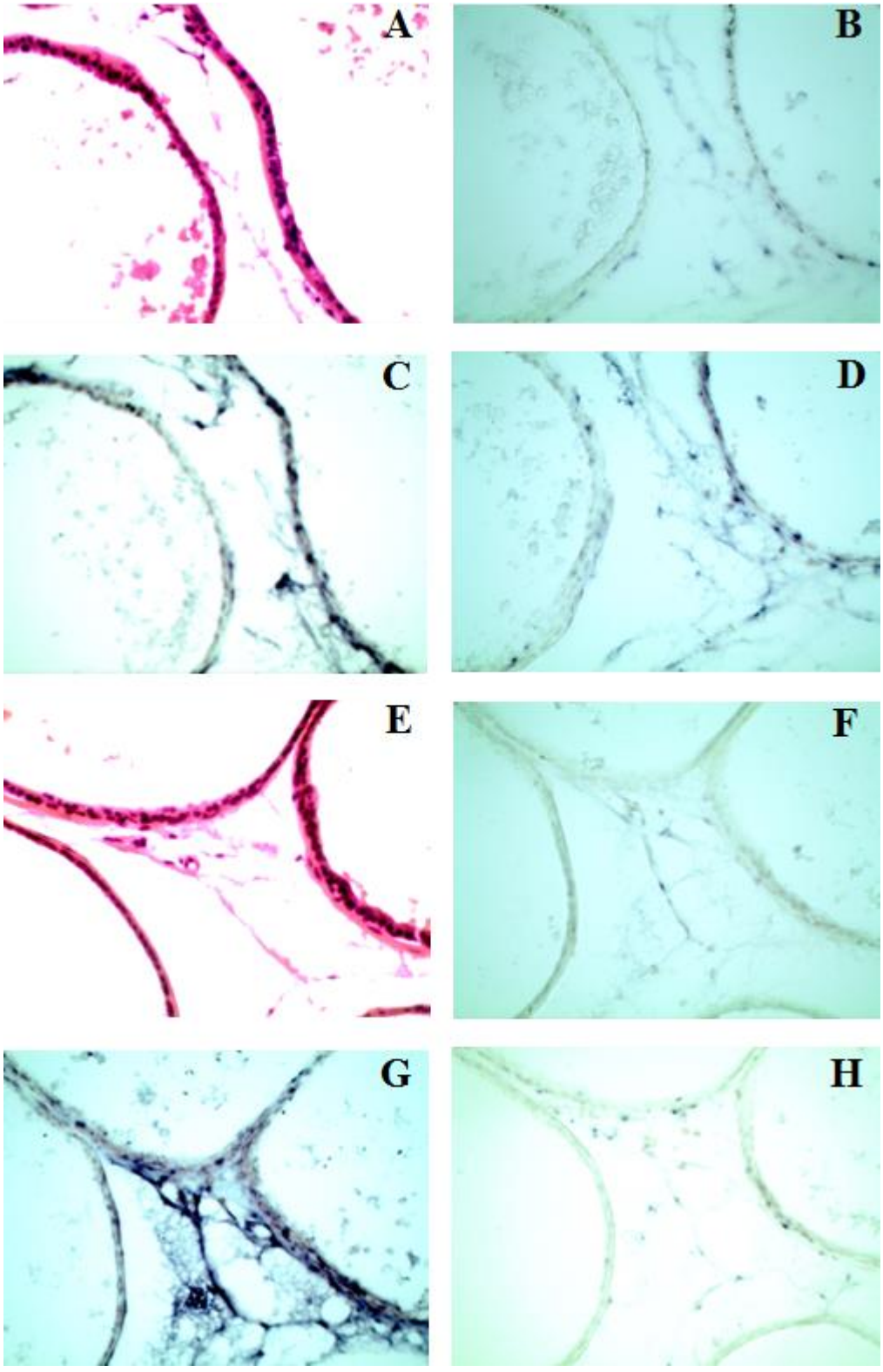

FIGURE 7. Results of the *in situ* hybridization. 40X magnification of the dorsolateral prostate. Picture taken with Olympus U-CMAD-2 camera. Results of both wild type (WT) and transgenic (TG) prostates are shown. (A) H&E staining of WT prostate. (B) Scrambled DNA staining of WT prostate. (C) U6 staining of WT prostate. (D) miR-32 staining of WT prostate. (E) H&E staining of TG prostate. (F) Scrambled DNA staining of TG prostate. (G) U6 staining of TG prostate. (H) miR-32 staining of TG prostate

5.2 Immunohistochemistry of Ki-67, Btg2, and Pten

5.2.1 Expression of Ki-67 in transgenic mouse prostate tissue

The expression of Ki-67 was investigated by comparing both WT and TG mouse prostates. In addition, the differences in both PAXgene fixation and formalin fixation were compared. The obtained results are shown in figure 8 as a 20X magnification of the ventral or dorsolateral prostate. The pictures were taken with the Olympus U-TV1X-2 camera system using the automated Objective Imaging Surveyor scanning program.

Figure 8A represents the Ki-67 expression of the PAXgene-fixed WT prostate. Figure 8B show the expression of Ki-67 in the PAXgene-fixed TG prostate. The expression of Ki-67 in formalin-fixed prostate is seen in figures 8C (WT) and 8D (TG). The brown staining of the nuclei is a representation of the Ki-67 expression in all the figures. The Ki-67 expression is marked with a black arrow in the figures. The blue-colored nuclei show no expression of Ki-67, as the blue color is a product of the Mayer's hematoxylin counterstaining.

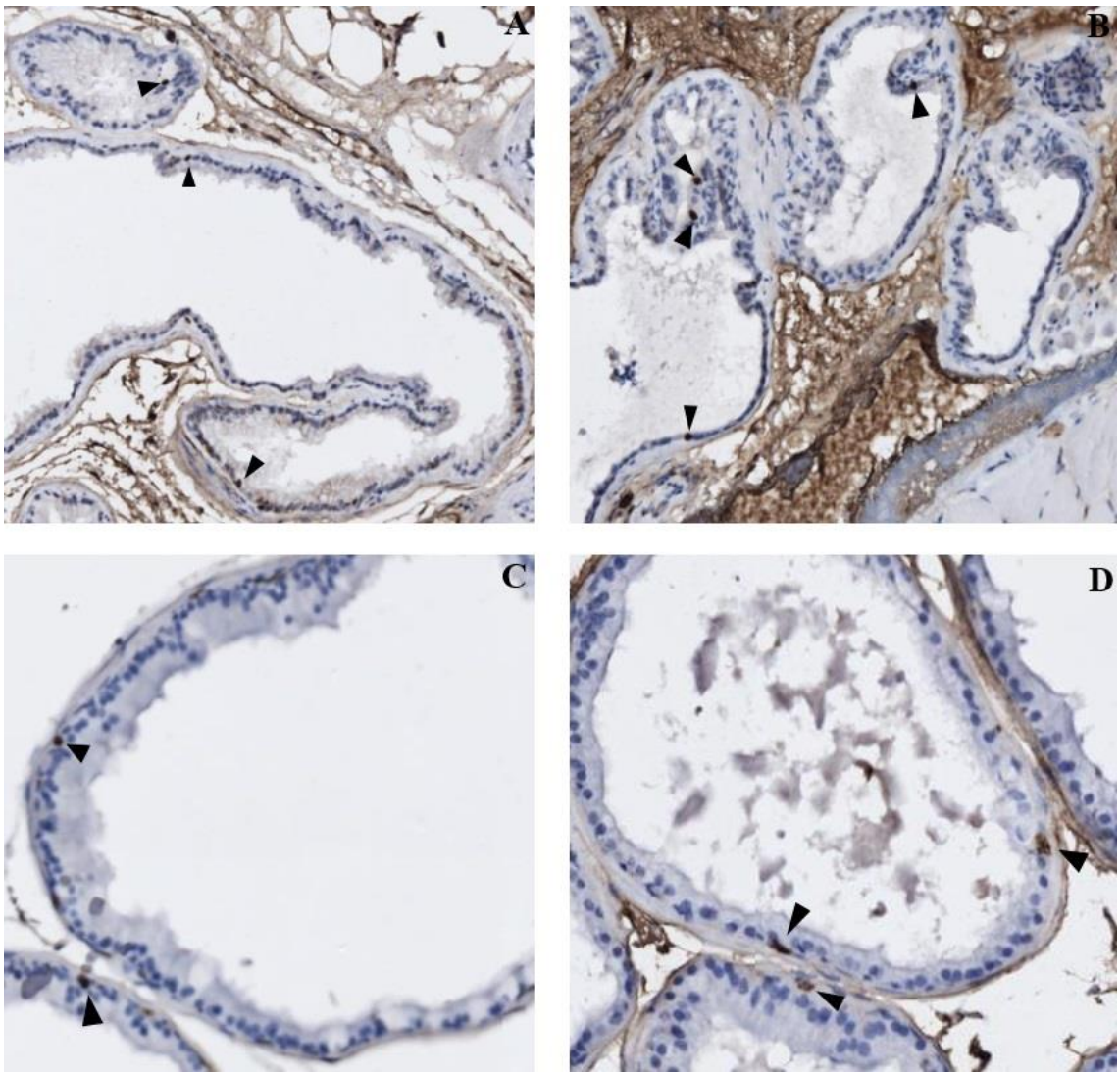

FIGURE 8. Results of the Ki-67 immunohistochemistry. 20X magnification. Picture taken with the Olympus U-TV1X-2 camera system. (A) PAXgene-fixed WT prostate. (B) PAXgene-fixed TG prostate. (C) Formalin-fixed WT prostate. (D) Formalin-fixed TG prostate. The brown color is a representation of Ki-67 expression. Ki-67 expressing nuclei are marked with arrows

5.2.2 Expression of Btg2 in transgenic mouse prostate tissue

The expression of Btg2 in transgenic mouse prostate tissue was investigated by comparing both WT and TG prostates. In addition, as previously, both fixatives were compared (PAXgene and formalin). The results are shown in figure 9 as a 20X magnification of the either ventral prostate, urethra, or ductus derefens. The pictures were taken with the Olympus U-TV1X-2 camera system using the automated Objective Imaging Surveyor scanning program.

The expression of Btg2 in PAXgene-fixed WT mouse is shown in figures 9A and 9B. Figure 9A represents the ventral prostate and 9B the urethra. The expression of Btg2 can be clearly seen, in figure 9A, as brown nuclear staining of the basal cells in the ventral prostate. The light-blue staining around the prostate represents the Mayer's hematoxylin counterstaining of the smooth muscle. The Btg2 staining of the urethra in figure 9B shows a well-defined difference in the staining of the inner epithelium of the urethra, as compared to the outer, blue-colored smooth muscle layer. This comparison was included to ensure the staining specificity between layers. The brown color, as seen on the edges, is caused by background staining.

Figures 9C and 9D represent the immunohistochemistry of the PAXgene-fixed TG mouse. Both the ventral prostate (9C) and the ductus deferens (9D) are shown. As previously, the basal cells are stained brown – an indication of Btg2 expression. The ductus deferens, shown in figure 9D, shows a clear difference in the staining of the different cell types. The Btg2 staining of the ductus deferens of both formalin-fixed WT and TG prostates is shown in figures 9E and 9F, respectively. When compared to the PAXgene fixation, no well-defined difference in the staining of the layers can be seen. As a result of the non-specific staining, no picture of the formalin-fixed ventral prostate is included.

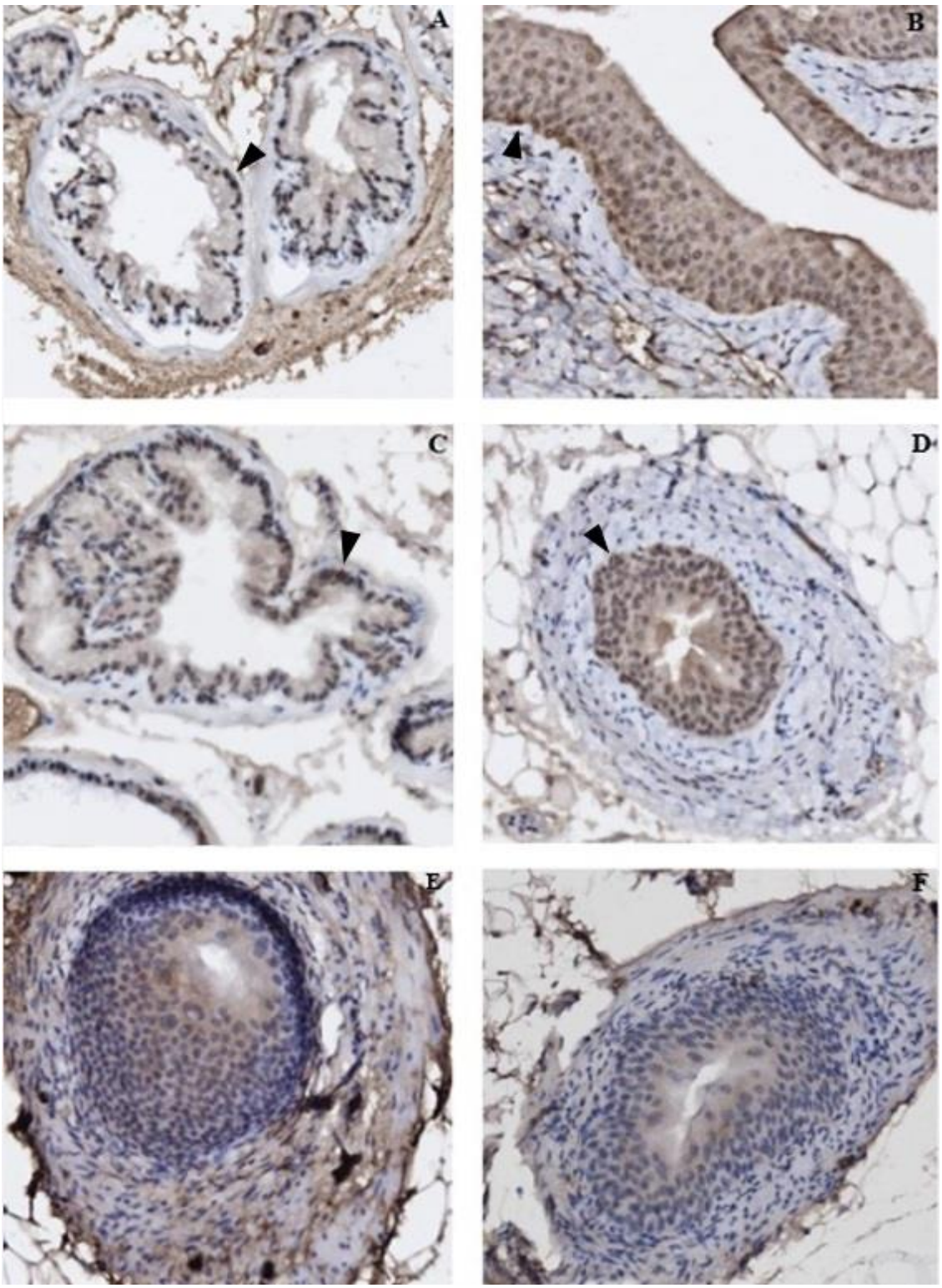

FIGURE 9. Results of the Btg2 immunohistochemistry. 20X magnification. Picture taken with the Olympus U-TV1X-2 camera system. (A) PAXgene-fixed WT prostate (ventral). (B) PAXgene-fixed WT urethra. (C) PAXgene-fixed TG prostate (ventral). (D) PAXgene-fixed TG ductus deferens. (E) Formalin-fixed WT ductus deferens. (F) Formalin-fixed TG ductus deferens. The brown color is a representation of Btg2 expression. The well-defined basal cell layer is marked with an arrow.

5.2.3 Expression of Pten in transgenic mouse prostate tissue

The expression of Pten in transgenic mouse prostate tissue was investigated in two parts: First, by comparing specificity of the staining in the urethra and second, by comparing the expression in ventral prostate of both WT and TG prostates. In addition, the staining of both formalin fixation and PAXgene fixation were compared. The results of the Pten expression in the urethra are shown in figure 10, and the ventral prostate in figure 11. The pictures in both figures 10 and 11 were taken as a 20X magnification with the Olympus U-TV1X-2 camera system with the help of the automated Objective Imagining Surveyor scanning program.

The expression of Pten in the urethra is shown in figure 10. In figures 10A–10D (PAXgene-fixed), a well-defined basal cell layer can be seen clearly as brown staining. This can be observed in both homozygous (*Pten*$^{+/+}$) WT and TG prostates (figures 10A and 10B, respectively). The same is observed in both heterozygous (*Pten*$^{+/-}$) WT and TG prostates (figures 10C and 10D, respectively). No clear difference in expression can be seen when comparing the homozygous prostates to the heterozygous ones. In comparison, the staining in figures 10E and 10F (formalin-fixed WT and TG prostate, respectively), is significantly more spread out: no well-defined basal cell layer can be seen. As a result, the formalin-fixed prostates were not included in the comparison in figure 11.

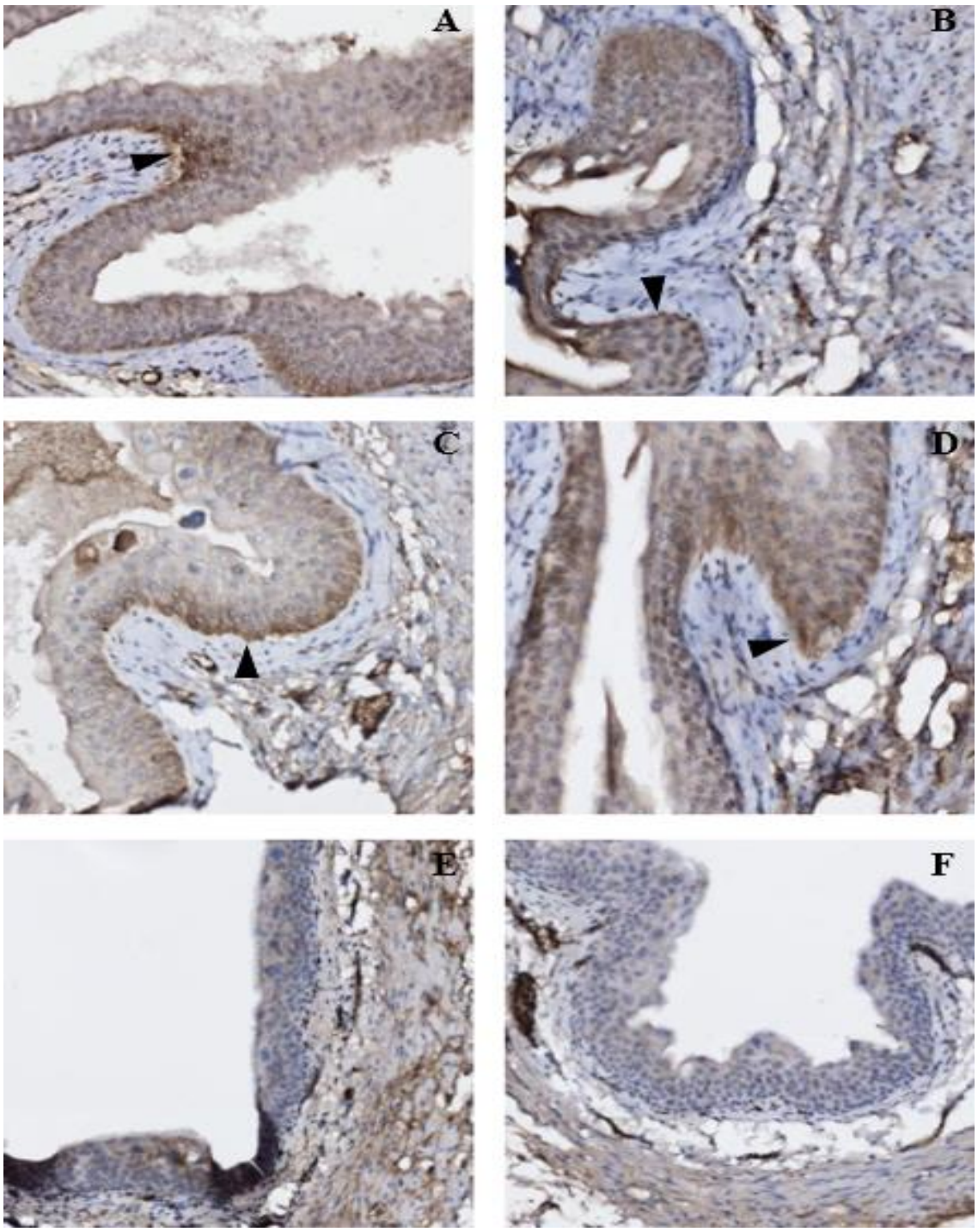

FIGURE 10. Results of the Pten immunohistochemistry. Comparison of staining specificity. 20X magnification of the urethra of both WT and TG prostates. Picture taken with the Olympus U-TV1X-2 camera system. Both PAXgene- and formalin-fixed prostates are included. (A) PAXgene-fixed homozygous (*Pten*$^{+/+}$) WT prostate. (B) PAXgene-fixed homozygous (*Pten*$^{+/+}$) TG prostate. (C) PAXgene-fixed heterozygous (*Pten*$^{+/-}$) WT prostate. (D) PAXgene-fixed heterozygous (*Pten*$^{+/-}$) TG prostate. (E) Formalin-fixed WT prostate. (F) Formalin-fixed TG prostate. The brown staining is a representation of Pten expression. The basal cell layer, stained brown, is marked with an arrow

In figure 11, the Pten expression of both homozygous and heterozygous prostates is compared. As established previously, specific expression of Pten is observed in the uroepithelium. Expression of Pten in the homozygous (*Pten*$^{+/+}$) WT prostate is shown in figure 11A, and in figure 11B for the homozygous (*Pten*$^{+/+}$) TG prostate. Heterozygous (*Pten*$^{+/-}$) Pten expression is shown in figure 11C for the WT prostate, and in figure 11D for the TG prostate.

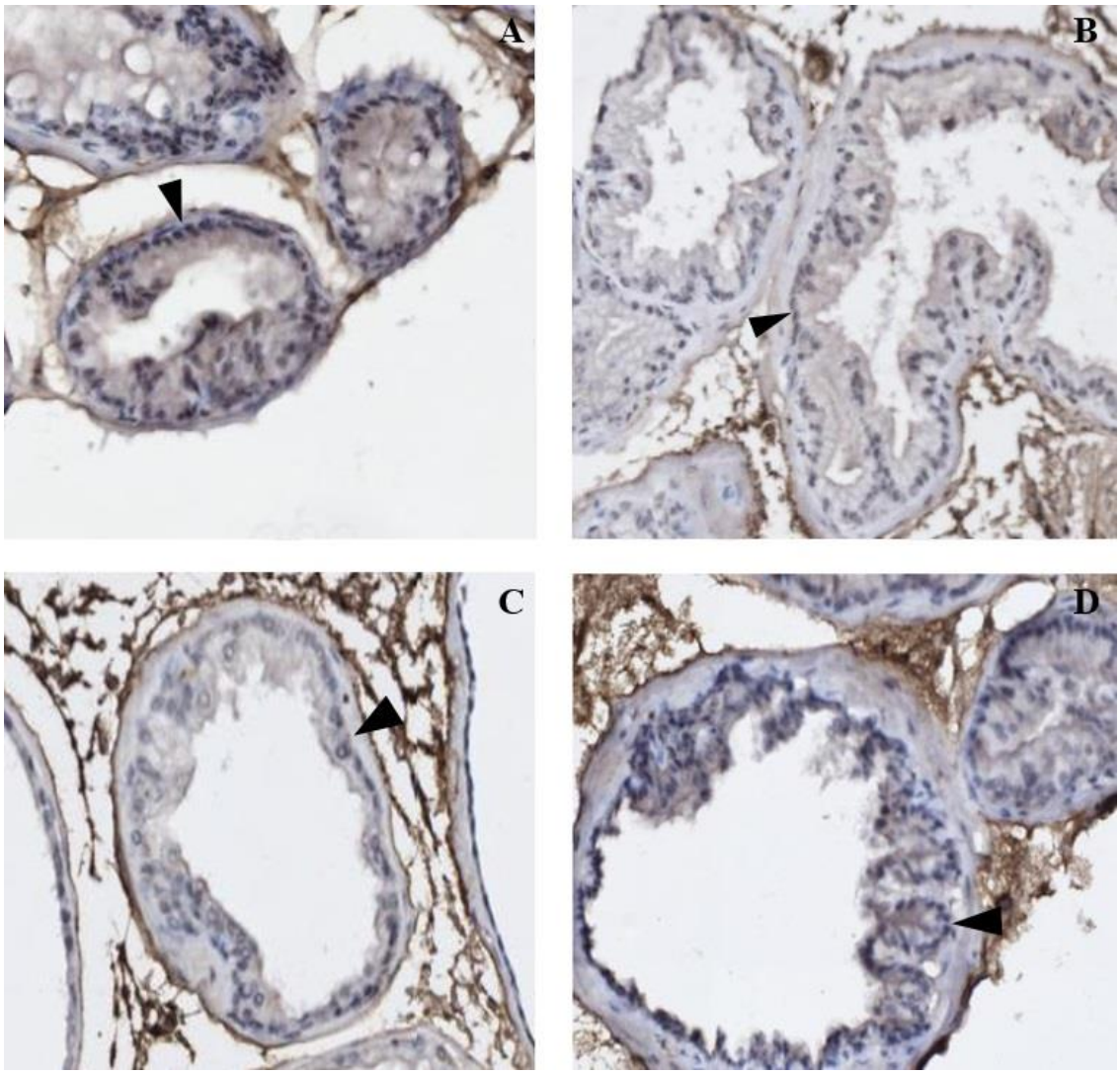

FIGURE 11. Results of the Pten immunohistochemistry. Comparison of Pten expression in PAXgene-fixed prostates. 20X magnification of the ventral prostate. Picture taken with the Olympus U-TV1X-2 camera system. (A) PAXgene-fixed homozygous (*Pten*$^{+/+}$) WT prostate. (B) PAXgene-fixed homozygous (*Pten*$^{+/+}$) TG prostate. (C) PAXgene-fixed heterozygous (*Pten*$^{+/-}$) WT prostate. (D) PAXgene-fixed heterozygous (*Pten*$^{+/-}$) TG prostate

6 DISCUSSION

The objective of the thesis was to study the expression of several promising biomarkers in transgenic mouse prostate tissue. The purpose of the thesis was to establish protocols for the *in situ* hybridization of miR-32 and the immunohistochemistry of Ki-67, Btg2, and Pten – and to study their expression. Two different fixatives were used during the study: 10% neutral buffered formalin and a commercial, alcohol-based PAXgene-fixative. Additionally, to evaluate the level of expression in transgenic mouse prostate tissue, the results were compared to those of wild type prostates. The prostates were collected from ethically treated mice which were euthanized by following strict guidelines for the welfare and use of animals in cancer research (Workman et al. 2010).

The Molecular Biology of Prostate Cancer Group had previously established a transgenic mouse line (ARR2PB-miR32), expressing miR-32 in the prostate epithelium. To increase the frequency of prostatic lesions, the mouse line was crossbred with mice heterozygous for *Pten* tumor suppressor gene. Thus, the miRNA ISH technique was used to evaluate the presence of miR-32 expression in the epithelium. The immunohistochemistry of Ki-67, Btg2, and Pten was further used to assist in the histopathological examination.

Based on the results shown in figure 7, specific miR-32 expression can be detected in both wild type and transgenic prostates. Results of both negative and positive controls further confirm the specificity of the miR-32 expression, as seen in figure 7. However, when comparing figures 7D and 7H, no clear difference in miR-32 expression can be seen between the WT and TG mouse prostates. Also, no direct comparison between prostate lobes can be made, as the staining was uneven in certain lobes of the prostate.

Uneven staining was further highlighted in the EDC-fixed samples, where entire sections of the prostate lobes were unstained. In addition, during the optimization attempts, EDC fixation seemed to cause a high amount of unspecific staining. This was observed in the controls as well, where the Scrambled DNA probe caused staining similar to specific miR-32 expression. Because of this, the results of the EDC-fixed miRNA ISH were not chosen for analysis, and are not included in figure 7.

As seen in figure 7, the expression of miR-32 is relatively low compared to U6 expression. In addition, the amount of background staining, as seen in figure 7G, is relatively high. High background staining can be caused, for example, by low hybridization temperature or insufficient stringent washes (Exiqon 2011, 28). Thus, increasing the duration of the final stringent wash from 45 minutes to at least 60 minutes should be attempted. Extra attention should be paid on preheating the buffer, as the first post-hybridization washing buffer was not properly preheated to + 37 °C. According to Exiqon (2011, 28), some non-specific staining can be explained by insufficient preheating.

According to Jones (2002, 565–566), the hybridization temperature should be 25 °C below the melting point. In the thesis, the hybridization temperature was + 37 °C, which is lower than the recommended value (+ 50 °C). A higher hybridization temperature might improve the level of miR-32 expression (Jones 2002, 566). Low hybridization temperature can even cause the probe to hybridize with similar sequences, leading to false results (Exiqon 2011, 26). In addition, due to the length of the miRNA ISH protocol, the hybridization time had to be adjusted from a few hours to overnight. This may have negative effects on the hybridization of the probe, since the hybridization durations in commercial miRNA ISH protocols are typically only one hour (Exiqon 2011, 20). Additionally, the optimization attempts included changes in the proteinase-K concentration while other conditions, such as the presence of EDC fixation, did not remain constant.

It is worth noting that RNAse contaminations are also possible, as the laboratory was not a proper RNAse-free environment, which may partially explain the lower-than-expected expression of miR-32, and some of the inconsistency with the results. In addition, as *in situ* hybridization is a highly challenging – and long – process, the short learning period and the time allotted to the technique might explain the varying results. In summary, a working miRNA ISH method was established, but due to the inconsistent miR-32 expression, further optimization and verification of the results should be attempted before moving to mice with confirmed prostatic lesions.

The immunohistochemistry in this thesis was focused on establishing methods for the detection of Ki-67, Btg2, and Pten. Successful methods were established during the project. The established protocol was identical for each antibody, thus providing a universal protocol for the immunohistochemistry of Ki-67, Btg2, and Pten. Even with the use of a

multi-species secondary antibody (anti-rabbit and anti-mouse), the obtained results show specificity with all tested antibodies.

Expression of Ki-67 in prostate tissue is linked to epithelial proliferation, which is a relative rare phenomenon in healthy prostate tissue. However, during prostate carcinogenesis, Ki-67 expression can be detected in the ventral prostate and the dorsolateral prostate. (Stanbrough et al. 2001.) As seen in figure 8, a few Ki-67 expressing nuclei can be detected in both PAXgene-fixed WT and TG prostates, as well as in the formalin-fixed WT and TG prostates. However, some background staining of the stroma is seen in figure 8 – especially in the PAXgene-fixed samples. Based on the results by Kap et al. (2011), some difference in the immunohistochemistry is to be expected between PFPE and FFPE samples, indicating that the background staining should not be compared too closely. Increasing the length of the washes should be attempted in order to try to remove some of the background staining. In addition, instead of the multi-species secondary antibody, a specific anti-rabbit antibody should be tested.

As established by Stanbrough et al. (2001), Ki-67 expression should be minimal in healthy prostate tissue, with few positive nuclei. None of the prostates in figure 8 show prostatic lesions, such as PIN, which is an indication that significant Ki-67 expression is not expected. In addition, the prostate epithelium shows no unspecific staining, with well-defined Ki-67 expressing nuclei. Based on these results, the established protocol for Ki-67 leads to specific staining in the prostate epithelium in both PAXgene- and formalin-fixed prostates. Thus, the protocol established here can be used for further Ki-67 staining in both PAXgene- and formalin-fixed prostates in the future, including samples with prostatic lesions.

BTG2 is an important tumor suppressor gene, responsible for many antiproliferative functions, necessary for normal cell function. BTG2 protein is a nuclear protein, and is mainly expressed in basal cells. (Kawamura-Tsuzuku et al. 2004; Ficazzola et al. 2001.) In figure 9, Btg2 expression can be clearly seen in the PAXgene-fixed prostate epithelium (9A and 9C), urethra (9B), and ductus deferens (9D). As observed in Ficazzola et al (2001), the expression of Btg2 in the prostate is mainly in the basal cells. This can be seen in figures 9A and 9C as well, where the Btg2 staining forms a clear basal cell layer inside the prostate epithelium.

The Btg2 expression is specific in both WT and TG prostates, clearly visible as well-defined borders between the epithelium (brown) and the smooth muscle (blue) in figure 9. However, as seen in figures 9E and 9F, the formalin-fixed prostates show unspecific staining in both the epithelium and the muscle layer. Based on these results, the established protocol shows specific Btg2 expression in the PAXgene-fixed prostates, but not in the formalin-fixed ones. Thus, the protocol established here can be used for further staining of Btg2 in PAXgene-fixed prostates, including prostates with prostatic lesions, such as PIN. However, more optimization should be attempted for formalin-fixed prostates.

The lack of specificity in the formalin-fixed prostates can be caused by multiple factors. Kap et al. (2011) observed that the formalin fixation and PAXgene fixation can have slight differences in the staining with immunohistochemistry. Thus, same conditions for the protocol might not apply for both fixation types. Based on the datasheet provided by Santa Cruz Biotechnology, there is no mention of a recommended technique for epitope unmasking. Because of this, the pH 9.0 HIER technique might not be optimal. As pH can matter greatly in the epitope unmasking, other buffers, such as the pH 6.0 citrate buffer should be tested (Kumar & Rudbeck 2009, 51–52). Specific anti-rabbit secondary antibody should be tested as well, instead of the multi-detection reagent. In addition, it is worth noting that the FFPE samples used here were stored for several months in the cold room, which may affect the results in immunohistochemistry. This should be tested by repeating the protocol with fresh tissue sections.

Phosphatase and tensin homolog (*PTEN*) is a well-established tumor suppressor gene. It is responsible for modulation the Akt-signaling pathway, thus having an important part in the regulation of cell cycle progression. (Celebi et al. 2000; Kanamori et al. 2001; Ohigashi et al. 2005.) According to Wang et al. (2003), Pten is expressed in the nuclear and cytoplasmic compartments of WT mice, and also in the prostate epithelium and the stromal cells. In figure 10, Pten expression can be clearly seen in the basal cells of the urethra. However, clear expression can only be seen in the PAXgene-fixed prostates (Figures 10A–10D). Thus, the formalin-fixed samples were not included in further analysis. In figure 11, a low level of Pten expression can be seen in all PAXgene-fixed samples, including the WT and TG prostates, as well as the homozygous and heterozygous variations.

As the ARR2PB-miR32 mouse line is crossbred with mice heterozygous for *Pten* tumor suppressor gene, Pten expression should be significantly lower in the transgenic mouse prostate (Blando et al. 2009). In figure 11 this difference cannot be clearly seen: the level of staining appears quite similar in all homozygous and heterozygous variants. However, it should be noted that immunohistochemistry is not a quantitative method, thus the intensity of the Pten expression between mouse lines should not be directly compared. As the expression of Pten in the formalin-fixed samples is not suitable (figures 10E and 10F), further optimization should be attempted. As with Ki-67 and Btg2, the pH 6.0 HIER method should be tested, along with the specific anti-rabbit secondary antibody. Based on these results, the established method here can be used for further Pten immunohistochemistry with PAXgene-fixed samples, including samples with prostatic lesions.

In conclusion, the objective and purpose of the thesis were largely accomplished. Successful immunohistochemical staining methods were obtained for Ki-67 with both formalin fixation and PAXgene fixation, for Btg2 with PAXgene fixation, and for Pten with PAXgene fixation. A working protocol for the *in situ* hybridization of miR-32 in PAXgene-fixed mice was also established here – although with a relatively weak signal and inconsistent staining. Ki-67 was shown to have a low level of specific expression in the prostate of both WT and TG mice, with no clear difference in expression. Btg2 was shown to be expressed in the basal cell layer of both WT and TG prostates. Specificity was confirmed by specific expression in the urethra (WT) and in the ductus deferens (TG). Expression of Pten was shown to be clearly visible in the basal cell layer of the urethra and prostate tissue in both WT and TG mice, with no clear difference in expression. And last, a low level of miR-32 expression was seen in the prostate epithelium of of both WT and TG mice.

In the future, the results obtained in this thesis can help the Prostate Cancer Research Group to investigate mouse lines with confirmed prostatic lesions, in order to investigate the role of these biomarkers in prostate carcinogenesis, and in the formation of castration-resistance. In addition, these methods will help clarify the success of the transgenic ARR2PB mouse line, established by the group. Hopefully, with further research on these putative biomarkers, clinical biomarkers of aggressive prostate cancer – and treatment options – are one step closer to reality.

REFERENCES

American Cancer Society. 2014. Prostate Cancer. Read 15.5.2014. Updated 12.3.2014. http://www.cancer.org/cancer/prostatecancer/detailedguide/prostate-cancer-what-is-prostate-cancer

Anderson, G. & Bancroft, J. 2002. Tissue processing and microtomy. In Bancroft, J. & Gamble, M. (ed.) Theory and Practice of Histological Techniques. 5th edition. Edinburgh: Churchill Livingstone.

Blando, J., Portis, M., Benavides, F., Alexander, A., Mills, G., Dave, B., Conti, C.J., Kim, J. & Walker, C.L. 2009. Pten Deficiency Is Fully Penetrant for Prostate Adenocarcinoma in C57BL/6 Mice via mTOR-Dependent Growth. The American Journal of Pathology 174 (5), 1869–1879.

Boiko, A.D., Porteous, S., Razorenova, O.V., Krivokrysenko, V.I., Williams, B.R. Gudkov, A.V. 2006. A systematic search for downstream mediators of tumor suppressor function of p53 reveals a major role of Btg2 in suppression of Ras-induced transformation. Genes & Development 20 (2), 236–252.

Bostwick, D.G. 1989. Prostatic intraepithelial neoplasia (PIN). Urology 34 (6), 16–22.

Bostwick, D.G., Liu, L., Brawer, M.K. & Qian, J. 2004. High-Grade Prostatic Intraepithelial Neoplasia. Reviews in Urology 6 (4), 171–179.

Bubendorf, L., Schöpfer, A., Wagner, U., Sauter, G., Moch, H., Willi, N., Gasser, T. & Mihatsch M.J. 2000. Metastatic patterns of prostate cancer: an autopsy study of 1,589 patients. Human Pathology 31 (5), 578–583.

Campisi, J. 2001. Cellular senescence as a tumor-suppressor mechanism. Trends in Cell Biology 11 (11), S27–31.

Celebi, J.T., Shendrik, I., Silvers, D.N. & Peacocke, M. 2000. Identification of Pten mutations in metastatic melanoma specimens. Journal of Medical Genetics 37 (9), 653–657.

Chen, Z., Trotman, L.C., Shaffer, D., Lin, H.K., Dotan, Z.A., Niki, M., Koutcher, J.A., Scher, H.I., Ludwig, T., Gerald, W., Cordon-Cardo, C. & Pandolfi P.P. 2005. Crucial role of p53-dependent cellular senescence in suppression of Pten-deficient tumorigenesis. Nature 436 (7051), 725–730.

Coppola, V., Musumeci, M., Patrizii, M., Cannistraci, A., Addario, A., Maugeri-Saccà, M., Biffoni, M., Francescangeli, F., Cordenonsi, M., Piccolo, S., Memeo, L., Pagliuca, A., Muto, G., Zeuner, A., De Maria, R. & Bonci, D. 2013. Btg2 loss and miR-21 upregulation contribute to prostate cell transformation by inducing luminal markers expression and epithelial-mesenchymal transition. Oncogene 32 (14), 1843–1853.

Croce, C.M. 2009. Causes and consequences of microRNA dysregulation in cancer. Nature Reviews Genetics 10 (10), 704–714.

Damber, J.E. & Aus, G. 2008. Prostate cancer. Lancet 371 (9625), 1710–1721.

De Bono, J.S., Logothetis, C.J., Molina, A., Fizazi, K., North, S., Chu, L., Chi, K.N., Jones, R.J., Goodman, O.B. Jr., Saad, F., Staffurth, J.N., Mainwaring, P., Harland, S., Flaig, T.W., Hutson, T.E., Cheng, T., Patterson, H., Hainsworth, J.D., Ryan, C.J., Sternberg, C.N., Ellard, S.L., Fléchon, A., Saleh, M., Scholz, M., Efstathiou, E., Zivi, A., Bianchini, D., Loriot, Y., Chieffo, N., Kheoh, T., Haqq, C.M. & Scher, H.I. 2011. Abiraterone and increased survival in metastatic prostate cancer. The New England Journal of Medicine 364 (21), 1995–2005.

Di Cristofano, A., Pesce, B., Cordon-Cardo, C. & Pandolfi, P.P. 1998. Pten is essential for embryonic development and tumour suppression. Nature Genetics 19 (4), 348–355.

Exiqon. 2011. miRCURY LNA™ microRNA ISH Optimization Kit (FFPE). Printed 24.6.2014. http://www.exiqon.com/ls/documents/scientific/mircury-lna-microrna-ish-optimization-kit-manual.pdf

Fang, Y.X. & Gao, W.Q. 2014. Roles of microRNAs during prostatic tumorigenesis and tumor progression. Oncogene 33 (2), 135–147.

Ficazzola, M.A., Fraiman, M., Gitlin, J., Wook, K., Melamed, J., Rubin, M.A. & Walden, P.D. 2001. Antiproliferative B cell translocation gene 2 protein is down-regulated post-transcriptionally as an early event in prostate carcinogenesis. Carcinogenesis 22 (8), 1271–1279.

Finnish Cancer Registry. 2009. Cancer in Finland 2006 and 2007. Helsinki: Cancer Society of Finland Publication No. 76.

Finnish Cancer Registry. 2014. Most common cancers in 2012, MALES. Read 15.5.2014. Updated 24.4.2014. http://stats.cancerregistry.fi/stats/eng/veng0020i0.html

Fisher, G., Zang, Z.H., Kudahetti, S., Møller, H., Scardino, P., Cuzick, J. & Berney, D.M. 2013. Prognostic value of Ki-67 for prostate cancer death in a conservatively managed cohort. British Journal of Cancer 108 (2), 271–277.

Freedland, S.J. & Moul, J.W. 2007. Prostate specific antigen recurrence after definite therapy. The journal of Urology 177 (6), 1985–1991.

Friedman, R.C., Farh, K.K., Burge, C.B. & Bartel, D.P. 2009. Most mammalian mRNAs are conserved targets of microRNAs. Genome Research 19 (1), 92–105.

Gerbi, S.A. & Lange, T.S. 2002. All Small Nuclear RNAs (snRNAs) of the [U4/U6.U5] Tri-snRNP Localize to Nucleoli; Identification of the Nucleolar Localization Element of U6 snRNA. Molecular Biology of the Cell 13 (9), 3123–3137.

Hermans, K.G., van Alewijk, D.C., Veltman, J.A., van Weerden, W., van Kessel, A.G. & Trapman, J. 2004. Loss of a small region around the Pten locus is a major chromosome 10 alteration in prostate cancer xenografts and cell lines. Genes, Chromosomes & Cancer 39 (3), 171–184.

Hopwood, D. 2002. Fixation and fixatives. In Bancroft, J. & Gamble, M. (ed.) Theory and Practice of Histological Techniques. 5th edition. Edinburgh: Churchill Livingstone.

Humphrey, P. 2004. Gleason grading and prognostic factors in carcinoma of the prostate. Modern Pathology 17 (3), 292–306.

Jalava, S.E., Urbanucci, A., Latonen, L., Waltering, K.K., Sahu, B., Jänne, O.A., Seppälä, J., Lähdesmäki, H., Tammela, T.L. & Visakorpi, T. 2012. Androgen-regulated miR-32 targets Btg2 and is overexpressed in castration-resistant prostate cancer. Oncogene 31 (41), 4460–4471.

Jones, M. 2002. Molecular pathology and in-situ hybridization. In Bancroft, J. & Gamble, M. (ed.) Theory and Practice of Histological Techniques. 5th edition. Edinburgh: Churchill Livingstone.

Kanamori, Y., Kigawa, J., Itamochi, H., Shimada, M., Takahashi, M., Kamazawa, S., Sato, S., Akeshima, R. & Terakawa, N. 2001. Correlation between loss of Pten expression and Akt phosphorylation in endometrial carcinoma. Clinical Cancer Research 7 (4), 892–895.

Kantoff, P.W., Higano, C.S., Shore, N.D., Berger, E.R., Small, E.J., Penson, D.F., Redfern, C.H., Ferrari, A.C., Dreicer, R., Sims, R.B., Xu, Y., Frohlich, M.W. & Schellhammer, P.F. 2010. Sipuleucel-T immunotherapy for castration-resistant prostate cancer. The New England Journal of Medicine 363 (5), 411–422.

Kap, M., Smedts, F., Oosterhuis, W., Winther, R., Christensen, N., Reischauer, B., Viertler, C., Groelz, D., Becker, K.F., Zatloukal, K., Langer, R., Slotta-Huspenina, J., Bodo, K., de Jong, B., Oelmuller, U. & Riegman, P. 2011. Histological assessment of PAXgene tissue fixation and stabilization reagents. PLoS One 6 (11), e27704.

Kawachi, M.H., Bahnson, R.R., Barry, M., Busby, J.E., Carroll, P.R., Carter, H.B., Catalona, W.J., Cookson, M.S., Epstein, J.I., Etzioni, R.B., Giri, V.N., Hemstreet, G.P. 3rd, Howe, R.J., Lange, P.H., Lilja, H., Loughlin, K.R., Mohler, J., Moul, J., Nadler, R.B., Patterson, S.G., Presti, J.C., Stroup, A.M, Wake, R. & Wei, J.T. 2010. NCCN clinical practice guidelines in oncology: prostate cancer early detection. Journal of the National Comprehensive Cancer Network: JNCCN 8 (2), 240–262.

Kawamura-Tsuzuku, J., Suzuki, T., Yoshida, Y. & Yamamoto, T. 2004. Nuclear localization of Tob is important for regulation of its antiproliferative activity. Oncogene 23 (39), 6630–6638.

Key, M. 2009. Immunohistochemistry Staining Methods. In Kumar, G. & Rudbech, L. (ed.) Immunohistochemical (IHC) Staining Methods. 5th edition. California: Dako North America.

Kumar, G. & Rudbech, L. 2009. Demasking of Antigens. In Kumar, G. & Rudbech, L. (ed.) Immunohistochemical (IHC) Staining Methods. 5th edition. California: Dako North America.

Li, H., Byeon, I.J., Ju, Y. & Tsai, M.D. 2004. Structure of human Ki67 FHA domain and its binding to a phosphoprotein fragment from hNIFK reveal unique recognition sites and new views to the structural basis of FHA domain functions. Journal of Molecular Biology 335 (1), 371–381.

Lin, S.L., Miller, J.D. & Ying, S.Y. 2006. Intronic microRNA (miRNA). Journal of Biomedicine & Biotechnology 2006 (4), 26818.

Mauxion, F., Faux, C. & Séraphin, B. 2008. The Btg2 protein is a general activator of mRNA deadenylation. The EMBO journal 27 (7), 1039–1048.

Miller, K. 2002. Immunocytochemical techniques. In Bancroft, J. & Gamble, M. (ed.) Theory and Practice of Histological Techniques. 5th edition. Edinburgh: Churchill Livingstone.

Montironi, R., Mazzucchelli, R., Lopez-Beltran, A., Cheng, L. & Scarpelli, M. 2007. Mechanisms of disease: high-grade prostatic intraepithelial neoplasia and other proposed preneoplastic lesions in the prostate. Nature Clinical Practice Urology 4 (6), 321–332.

NCBI Reference Sequence Database. 2013. Mus musculus microRNA 32 (Mir32), microRNA. Read 23.5.2014. http://www.ncbi.nlm.nih.gov/nuccore/NR_029789.1

Nguyen, H.G., Yang, J.C., Kung, H.J., Shi, X.B., Tilki, D., Lara, P.N. Jr., Devere White, R.W., Gao, A.C. & Evans, C.P. 2014. Targeting autophagy overcomes Enzalutamide resistance in castration-resistant prostate cancer cells and improves therapeutic response in a xenograft model. Oncogene 33 (36), 4521–4530.

Nielsen, B. 2012. MicroRNA In Situ Hybridization. In Fan, J.B. (ed.) Next-Generation MicroRNA Expression Profiling Technology. New York: Humana Press.

Ohigashi, T., Mizuno, R., Nakashima, J., Marumo, K. & Murai, M. 2005. Inhibition of Wnt Signaling Downregulates Akt Activity and Induces Chemosensitivity in Pten-Mutated Prostate Cancer Cells. The Prostate 62 (1), 61–8.

Pacelli, A. & Bostwick, D.G. 1997. Clinical significance of high-grade prostatic intraepithelial neoplasia in transurethral resection specimens. Urology 50 (3), 355–359.

Pena, J.T.G., Sohn-Lee, C., Rouhanifard, S.H., Ludwig, J., Hafner, M., Mihailovic, A., Lim, C., Holoch, D., Berninger, P., Zavolan, M. & Tuschl, T. 2009. miRNA *in situ* hybridization in formaldehyde and EDC-fixed tissues. Nature Methods 6 (2), 139–141.

Pierorazio, P.M., Guzzo, T.J., Han, M., Bivalacqua, T.J., Epstein, J.I., Schaeffer, E.M., Schoenberg, M., Walsh, P.C. & Partin, A.W. 2010. Long-Term Survival after Radical Prostatectomy for men with High Gleason Sum in the Pathological Specimen. Urology 76 (3), 715–721.

Renshaw, S. 2006. Immunochemical staining techniques. Immunohistochemistry: Methods Express. United Kingdom: Scion Publishing Ltd.

Ross, M. & Pawlina, W. 2011. Histology. A Text and Atlas, with Correlated Cell and Molecular Biology. 6th edition. Baltimore: Lippincott Williams & Wilkins.

Sato, M., Kojima, M., Nagatsuma, A.K., Nakamura, Y., Saito, N. & Ochiai, A. 2014. Optimal fixation for total preanalytic phase evaluation in pathology laboratories. A comprehensive study including immunohistochemistry, DNA, and mRNA assays. Pathology International 64 (5), 209–216.

Scher, H.I., Fizazi, K., Saad, F., Taplin, M.E., Sternberg, C.N., Miller, K., de Wit, R., Mulders, P., Chi, K.N., Shore, N.D., Armstrong, A.J., Flaig, T.W., Fléchon, A., Mainwaring, P., Fleming, M., Hainsworth, J.D., Hirmand, M., Sleby, B., Seely, L. & De Bono, J.S. 2012. Increased survival with enzalutamide in prostate cancer after chemotherapy. The New England Journal of Medicine 367 (13), 1187–1197.

Shappell, S.B., Thomas, G.V., Roberts, R.L., Herbert, R., Ittmann, M.M., Rubin, M.A., Humphrey, P.A., Sundberg, J.P., Rozengurt, N., Barrios, R., Ward, J.M. & Cardiff, R. D. 2004. Prostate pathology of genetically engineered mice: definitions and classification. The consensus report from the Bar Harbor meeting of the Mouse Models of Human Cancer Consortium Prostate Pathology Committee. Cancer Research 64 (6), 2270–2305.

Shen, M.M. & Abate-Shen, C. 2010. Molecular genetics of prostate cancer: new prospects for old challenges. Genes & Development 24 (18), 1967–2000.

Sigma-Aldrich. 2002. Hematoxylin & eosin (The Routine Stain). Printed 9.6.2014. http://www.sigmaaldrich.com/img/assets/7361/Primer-H&Emay04.pdf

Stanbrough, M., Leav, I., Kwan, P.W., Bubley, G.J. & Balk, S.P. 2001. Prostatic intraepithelial neoplasia in mice expressing an androgen receptor transgene in prostate epithelium. Proceedings of the National Academy of Sciences of the United States of the America 98 (19), 10823–10828.

Thermo Scientific. 2014. Pierce NBT/BCIP Substrates and Solutions. Read 12.6.2014. http://www.piercenet.com/product/nbt-bcip-substrates-solutions

Thomsen, R., Nielsen, P.S. & Jensen, T.H. 2005. Dramatically improved RNA in situ hybridization signals using LNA-modified probes. RNA 11 (11), 1745–1748.

Urbanucci, A., Sahu, B., Seppälä, J., Larjo, A., Latonen, L.M., Waltering, K.K., Tammela, T.L., Vessella, R.L., Lähdesmäki, H., Jänne, O.A. & Visakorpi, T. 2012. Oncogene 31 (17), 2153–2163.

Urruticoechea, A., Smith, I.E. & Dowsett, M. 2005. Proliferation marker Ki-67 in early breast cancer. Journal of Clinical Oncology 23 (28), 7212–7220.

Van der Kwast, T.H. 2014. Prognostic prostate tissue biomarkers of potential clinical use. Virchows Archiv 464 (3), 293–300.

Waltering, K.K., Porkka, K.P., Jalava, S.E., Urbanucci, A., Kohonen, P.J., Latonen, L.M., Kallioniemi, O.P., Jenster, G. & Visakorpi, T. 2011. Androgen regulation of micro-RNAs in prostate cancer. Prostate 71 (6), 604–614.

Wang, S., Gao, J., Lei, Q., Rozengurt, N., Pritchard, C., Jiao, J., Thomas, G.V., Li, G., Roy-Burman, P., Nelson, P.S., Liu, X. & Wu, H. 2003. Prostate-specific deletion of the murine Pten tumor suppressor gene leads to metastatic prostate cancer. Cancer Cell 4 (3), 209–221.

Wilson, I. & Gamble, M. 2002. The hematoxylins and eosin. In Bancroft, J. & Gamble, M. (ed.) Theory and Practice of Histological Techniques. 5th edition. Edinburgh: Churchill Livingstone.

Woenckhaus, J. & Fenic, I. 2008. Proliferative inflammatory atrophy: a background lesion of prostate cancer? Andrologia 40 (2), 134–137.

Workman, P., Aboagye, E.O., Balkwill, F., Balmain, A., Bruder, G., Chaplin, D.J., Double, J.A., Everitt, J., Farningham, D.A., Glennie, M.J., Kelland, L.R., Robinson, V., Stratford, I.J., Tozer, G.M., Watson, S., Wedge, S.R., Eccles, S.A. & Committee of the National Cancer Research Institute. 2010. Guidelines for the welfare and use of animals in cancer research. British journal of cancer 102 (11), 1555–1577.

Wu, W., Yang, J., Feng, X., Wang, H., Ye, S., Yang, P., Tan, W., Weig, G. & Zhou, Y. 2013. MicroRNA-32 (miR-32) regulates phosphatase and tensin homologue (Pten) expression and promotes growth, migration, and invasion in colorectal carcinoma cells. Molecular Cancer 12 (30), doi:10.1186/1476-4598-12-30.

Yoshimoto, M., Cunha, I.W., Coudry, R.A., Fonseca, F.P., Torres, C.H., Soares, F.A. & Squire J.A. 2007. FISH analysis of 107 prostate cancers shows that Pten genomic deletion is associated with poor clinical outcome. British Journal of Cancer 97 (5), 678–685.

Yoshimoto, M., Cutz, J.C., Nuin, P.A., Joshua, A.M., Bayani, J., Evans, A.J., Zielenska, M. & Squire J.A. 2006. Interphase FISH analysis of Pten in histologic sections shows genomic deletions in 68% of primary prostate cancer and 23% of high-grade prostatic intra-epithelial neoplasias. Cancer Genetics and Cytogenetics 169 (2), 128–137.

APPENDICES

Attachment 1. Reagent list for the *in situ* hybridization

Solution	Content
Proteinase-K	5.0 µg/ml Proteinase-K (Sigma-Aldrich) in Proteinase-K buffer
Proteinase-K buffer	5 mM Tris-HCl, 1 mM EDTA, 1 mM NaCl in DEPC-treated H_2O (autoclaved)
Glycine buffer	0.2% Glycine in PBS
Imidazole buffer	0.13 M 1-methylimidazole, 300 mM NaCl in DEPC-treated H_2O pH 8.0
Prehybridization buffer	50% formamide, 5X SSC
Hybridization buffer	50% formamide, 5X SSC, 10% Dextran Sulphate Sodium, 500 µg/ml Salmon sperm (denatured), 0.02% BSA
U6 probe	0.5 nM U6 probe (Exiqon, LOT: 63249191) in hybridization buffer. Probe denatured before use
Scrambled DNA probe	25 nM Scrambled DNA probe (Exiqon, LOT: 63249176) in hybridization buffer. Probe denatured before use
miR-32 probe	25 nM hsa-miR-32 probe (Exiqon, batch 152466) in hybridization buffer. Probe denatured before use
1st Stringency wash buffer	5X SSC, 50% formamide mix
2nd Stringency wash buffer	2X SSC, 50% formamide mix
3rd Stringency wash buffer	0.2X SSC, 50% formamide mix
10X blocking solution	10% Blocking reagent in Maleic acid buffer (Roche)
1X blocking solution	10X blocking solution diluted to 1:10 with 1X Maleic acid buffer
Anti-DIG-HRP	1:800 dilution of Anti-DIG-HRP in 1X blocking solution
DIG Amplification working solution 1:50	1:800 dilution of DIG amplification stock solution in dilution reagent (PerkinElmer)
Anti-DIG-AP	1:800 dilution of Anti-DIG-AP in 1X b locking solution, 2% sheep serum
AP substrate working solution	1:50 dilution of NBT/BCIP stock solution (Roche) in 0.1 M Tris-HCl, 0.1 M NaCl pH 8.5
KTBT (AP stop solution)	50 mM Tris-HCl, 150 mM NaCl, 10 mM KCl in DEPC-treated H_2O (autoclaved)

Attachment 2. Reagent list for the immunohistochemistry

Solution	Content
Endogenous Peroxidase 3% H_2O_2	Commercial (VWR, LOT: 12B240024)
TE buffer	10 mM Tris Base, 1 mM EDTA, 0.05% Tween 20, pH 9.0
Ki-67 antibody (MM1)	Novocastra™ Lyophilized Mouse Monoclonal Antibody Ki67 Antigen MM1 (Leica Biosystems, LOT: 111870)
Ki-67 antibody (SP6)	Anti-Ki-67 Clone: SP6, Lab Vision Rabbit Monoclonal Antibody (Thermo Scientific, LOT: 9106S 1010G)
Btg2 antibody	Btg2 (H-50): sc-33775 (Santa Cruz Biotechnology) rabbit polyclonal antibody
Pten antibody	Pten (138G6) Rabbit mAb (Cell Signaling Technology) rabbit monoclonal antibody (LOT: 12)
Primary antibody diluent	Normal Antibody Diluent (Immunologic, LOT: 211013)
Secondary antibody	Histofine Simple Stain MAX PO (multi) Universal Immuno-peroxidase Polymer Anti-Mouse and -Rabbit (Nichirei Biosciences, LOT: H1312-1)
ImmPACT DAB substrate	1:40 dilution of ImmPACT DAB Chromogen in DAB Diluent (Vector Laboratories, LOT: Z0703)
Counterstain solution	Mayer's Hematoxylin (Histolab)